Prostaglandins regulate nuclear localization of Fascin and its function in nucleolar architecture

Christopher M. Groen[a], Asier Jayo[b], Maddy Parsons[b], and Tina L. Tootle[a]
[a]Anatomy and Cell Biology, Carver College of Medicine, University of Iowa, Iowa City, IA 52242; [b]Randall Division of Cell and Molecular Biophysics, King's College London, London SE1 1UL, United Kingdom

ABSTRACT **Fascin, a highly conserved actin-bundling protein, localizes and functions at new cellular sites in both *Drosophila* and multiple mammalian cell types. During *Drosophila* follicle development, in addition to being cytoplasmic, Fascin is in the nuclei of the germline-derived nurse cells during stages 10B–12 (S10B–12) and at the nuclear periphery during stage 13 (S13). This localization is specific to Fascin, as other actin-binding proteins, Villin and Profilin, do not exhibit the same subcellular distribution. In addition, localization of fascin1 to the nucleus and nuclear periphery is observed in multiple mammalian cell types. Thus the regulation and function of Fascin at these new cellular locations is likely to be highly conserved. In *Drosophila*, loss of prostaglandin signaling causes a global reduction in nuclear Fascin and a failure to relocalize to the nuclear periphery. Alterations in nuclear Fascin levels result in defects in nucleolar morphology in both *Drosophila* follicles and cultured mammalian cells, suggesting that nuclear Fascin plays an important role in nucleolar architecture. Given the numerous roles of Fascin in development and disease, including cancer, our novel finding that Fascin has functions within the nucleus sheds new light on the potential roles of Fascin in these contexts.**

Monitoring Editor
Julie Brill
The Hospital for Sick Children

Received: Sep 17, 2014
Revised: Mar 17, 2015
Accepted: Mar 18, 2015

INTRODUCTION

The actin-binding protein Fascin has been widely studied for its ability to bundle or cross-link parallel actin filaments into tight bundles. This conserved bundling function is critical for the formation of many morphologically identical cellular structures from *Drosophila* to mammals. Fascin is of particular interest in mammalian systems, as it is increasingly cited as a biomarker for aggressive cancers (Hashimoto *et al.*, 2005). In cancer cells, Fascin is important for the formation of elongated actin bundles necessary for the generation of filopodia (Vignjevic, 2006; Hashimoto *et al.*, 2007) and invadopodia (Li *et al.*, 2010; Schoumacher *et al.*, 2010). Of importance, these bundles are morphologically similar to those observed in *Drosophila* nurse cells (Huelsmann *et al.*, 2013). Novel interactions between Fascin and proteins such as Rab35 (Zhang *et al.*, 2009), protein kinase C (PKC; Anilkumar *et al.*, 2003; Hashimoto *et al.*, 2007), Lim kinases (Jayo *et al.*, 2012), and Daam1 (Jaiswal *et al.*, 2013) have highlighted new potential modes of action for Fascin, independent of its traditional role as an actin bundler. Recent work has also shown that Fascin plays critical roles in filopodial formation independent of its actin cross-linking function in these structures (Zanet *et al.*, 2012), promotes Enabled processivity in vitro (Winkelman *et al.*, 2014), and negatively regulates myosin-dependent contractility in cancer cells (Elkhatib *et al.*, 2014). In addition, these studies illustrate that Fascin localization and protein–protein interactions are important mechanisms of Fascin regulation.

Late-stage *Drosophila* oogenesis provides an excellent model system with which to analyze both actin cytoskeletal dynamics and the activities of actin-binding proteins. Oogenesis consists of 14 morphologically defined stages (reviewed in Spradling, 1993), and stages 10B (S10B) through 14 (S14) require dynamic remodeling of the actin cytoskeleton that occurs due to the coordinated efforts of a number of actin-binding proteins (reviewed in Hudson and Cooley, 2002). At S10B, the follicle consists of a single oocyte that is approximately half of the follicle volume and 15 germline-derived support, or nurse, cells. Within the nurse cells, an array of radially aligned actin filament bundles form at the nurse cell membranes and extend inward toward the nucleus to form a cage

This article was published online ahead of print in MBoC in Press (http://www.molbiolcell.org/cgi/doi/10.1091/mbc.E14-09-1384) on March 25, 2015.
Address correspondence to: Tina L. Tootle (tina-tootle@uiowa.edu).
Abbreviations used: F-actin, filamentous actin; LINC, Linker of Nucleoskeleton and Cytoskeleton; PG, prostaglandin; RFI, relative fluorescence intensity; S8, 9, 10A, 10B, 11, 12, 13, 14, specific stages of oogenesis; WGA, wheat germ agglutinin.

(Guild *et al.*, 1997; Huelsmann *et al.*, 2013). During S11, these bundles hold the nuclei in place as the network of cortical actin contracts and squeezes the nurse cell cytoplasm into the growing oocyte in a process called nurse cell dumping (Wheatley *et al.*, 1995). By S12, dumping is completed, and through S13, the nurse cells continue to shrink and die, leaving a mature S14 follicle that is composed of a single oocyte surrounded by a follicular epithelium.

Fascin (Drosophila Singed, Sn) is necessary for the formation of actin bundles during S10B and is thus critical for the process of nurse cell dumping (Cant *et al.*, 1994; Cant and Cooley, 1996). These findings make late-stage oogenesis an excellent model with which to uncover novel functions of Fascin and determine the mechanisms by which this regulation occurs. Indeed, this model was used to elucidate Fascin's bundling-independent role in promoting actin bundle formation and filopodium initiation (Zanet *et al.*, 2012) and in regulating cortical actin integrity (Groen *et al.*, 2012). We recently showed that Fascin is a novel downstream target of prostaglandin (PG) signaling during *Drosophila* oogenesis (Groen *et al.*, 2012).

PGs are short-lived lipids that act as autocrine or paracrine signaling molecules. PGs regulate a wide range of biological processes, including pain, inflammation, fertility, and cancer development (reviewed in Funk, 2001). PG synthesis begins with the conversion of arachidonic acid to the precursor prostaglandin, PGH_2, by cyclooxygenase (COX) enzymes, the targets of nonsteroidal anti-inflammatory drugs such as aspirin. Individual synthases convert PGH_2 into biologically active PGs, which signal through G protein–coupled receptors to mediate their downstream effects (reviewed in Tootle, 2013). One of the downstream targets of PG signaling is the actin cytoskeleton, which has been shown in vitro to be regulated in a cell type– and PG-dependent manner (Peppelenbosch *et al.*, 1993; Tamma *et al.*, 2003; Bulin *et al.*, 2005). The mechanisms by which PGs regulate the actin cytoskeleton, however, are poorly understood (Pierce, 1999; Dormond *et al.*, 2002; Birukova *et al.*, 2007). We hypothesize that a PG elicits a signaling cascade that regulates Fascin activity; how direct this regulation is and its precise mechanisms remain unknown.

Here we describe a novel function of Fascin at previously undescribed sites of Fascin localization. In *Drosophila*, Fascin, in addition to being cytoplasmic, localizes to the nuclei of the nurse cells during S10B–12 and to the nuclear periphery during S13. This localization is specific to Fascin and is dependent upon both PG signaling and completion of nurse cell dumping. We also show that fascin1 localizes within the nucleus and proximal to the nuclear envelope in a range of mammalian cell types, suggesting that these localizations likely reflect conserved functions of Fascin. Finally, we show that Fascin affects nucleolar morphology in both *Drosophila* and mammalian cells. Although the nucleolus is best known for its role as the site of ribosome biogenesis, it has many other functions (reviewed in Boisvert *et al.*, 2007; Ruggero, 2012; Hein *et al.*, 2013). Indeed, proteomic analysis of the nucleolus reveals a dynamic proteome that responds to the environment and implicates the nucleolus in regulating cell proliferation, differentiation, senescence, apoptosis, and coordination of cellular response to stress (Andersen *et al.*, 2002; Scherl *et al.*, 2002; Coute *et al.*, 2006; Leung *et al.*, 2006; Ahmad *et al.*, 2009).

Our data reveal that Fascin localizes to new cellular locations—the nucleus and nuclear periphery—in multiple contexts and suggest a novel function for Fascin in regulating nucleolar architecture. In the future, it will be important to determine the nucleolar role that Fascin plays during both developmental processes and cancer, and how Fascin modulation of nucleolar structure affects its functions.

RESULTS

Fascin localizes to the nucleus in *Drosophila* nurse cells

Fascin localization was examined during *Drosophila* oogenesis using the sn 7C antibody (Cant *et al.*, 1994). Although the sn 7C antibody was raised against full-length Fascin protein, Cant *et al.* (1994) demonstrated that the antibody does not recognize Fascin bound within canonical actin bundles. Our images show that the non–actin-bundled form of Fascin localized to the nurse cell nuclei in two distinct pools—within the nucleus and at the periphery—and that this localization changed throughout late-stage oogenesis. Although Fascin was largely cytoplasmic during S10B, it was also found in nuclei at a low level (Figure 1A and Supplemental Figure S1, A–A″). As development proceeds through and completes nurse cell dumping (S11 and S12), our images reveal that Fascin levels increased within the nucleus and began to accumulate around the nuclear periphery while still maintaining a large cytoplasmic pool (Figure 1, B and C, and Supplemental Figure S1, B–C″). Conversely, S13 follicles exhibited strong Fascin localization around the nuclear periphery and relatively low levels within the nuclei (Figure 1, D and E, and Supplemental Figure S1, D–D″).

Because the observed subcellular localization of Fascin was unexpected, we took a number of additional approaches to examine Fascin localization. First, to confirm that the immunofluorescent signal we observed was specific to Fascin, we examined *fascin*-null mutants. No signal was observed in these mutants using the sn 7C antibody by either immunofluorescence (Supplemental Figure S2, E–H compared with A–D) or Western blot (Supplemental Figure S2I), confirming that the nuclear signal observed in wild-type follicles was specific to the Fascin protein. Furthermore, we analyzed the subcellular distribution of green fluorescent protein (GFP)–tagged Fascin in live follicles coexpressing monomeric red fluorescent protein (mRFP)–tagged Nucleoporin107 (mRFP-Nup107) to mark the nuclear envelope. Like endogenous Fascin, GFP-Fascin localized within the nuclei during S10B–S12 (Figure 1, F–H, and Supplemental Movies S1 and S2) and to the nuclear periphery at S13 (Figure 1, I and J). We also used fluorescence recovery after photobleaching (FRAP) to analyze GFP-Fascin dynamics during S10B. When a whole nucleus is bleached, the GFP-Fascin signal recovers, on average, in 8 min (recovery halftime average of 53 s) to 85% of its original fluorescence intensity (Figure 2, A and B, and Supplemental Movie S3). In addition, if only a small portion of a nucleus is bleached, fluorescence recovers, on average, in 10 s (average recovery halftime of 5 s) to 85% of original intensity (Figure 2, C and D, and Supplemental Movie S4). These data indicate that Fascin is dynamically transported into the nucleus and that fascin is mobile within the nucleus during S10B. Fascin is a 55-kDa protein (Cant *et al.*, 1994) and is too large to passively diffuse through nuclear pore complexes, which have a limit of ~40 kDa for passive diffusion (Keminer and Peters, 1999). These data suggest that Fascin localization within the nucleus is regulated.

Fascin localizes to the nucleus and nuclear periphery in mammalian cells

The role of Fascin as an actin-bundling protein is highly conserved between *Drosophila* and mammalian cells (reviewed in Edwards and Bryan, 1995). Indeed, Fascin function and phosphorylation regulate a number of actin-dependent processes in many different human cancer cells, including adhesion and migration (Hashimoto *et al.*, 2007; Li *et al.*, 2010; Jayo *et al.*, 2012). To define whether Fascin localization to the nucleus and nuclear periphery was conserved in mammalian cells, we stained a range of cells for endogenous fascin1 and carefully analyzed its subcellular distribution by

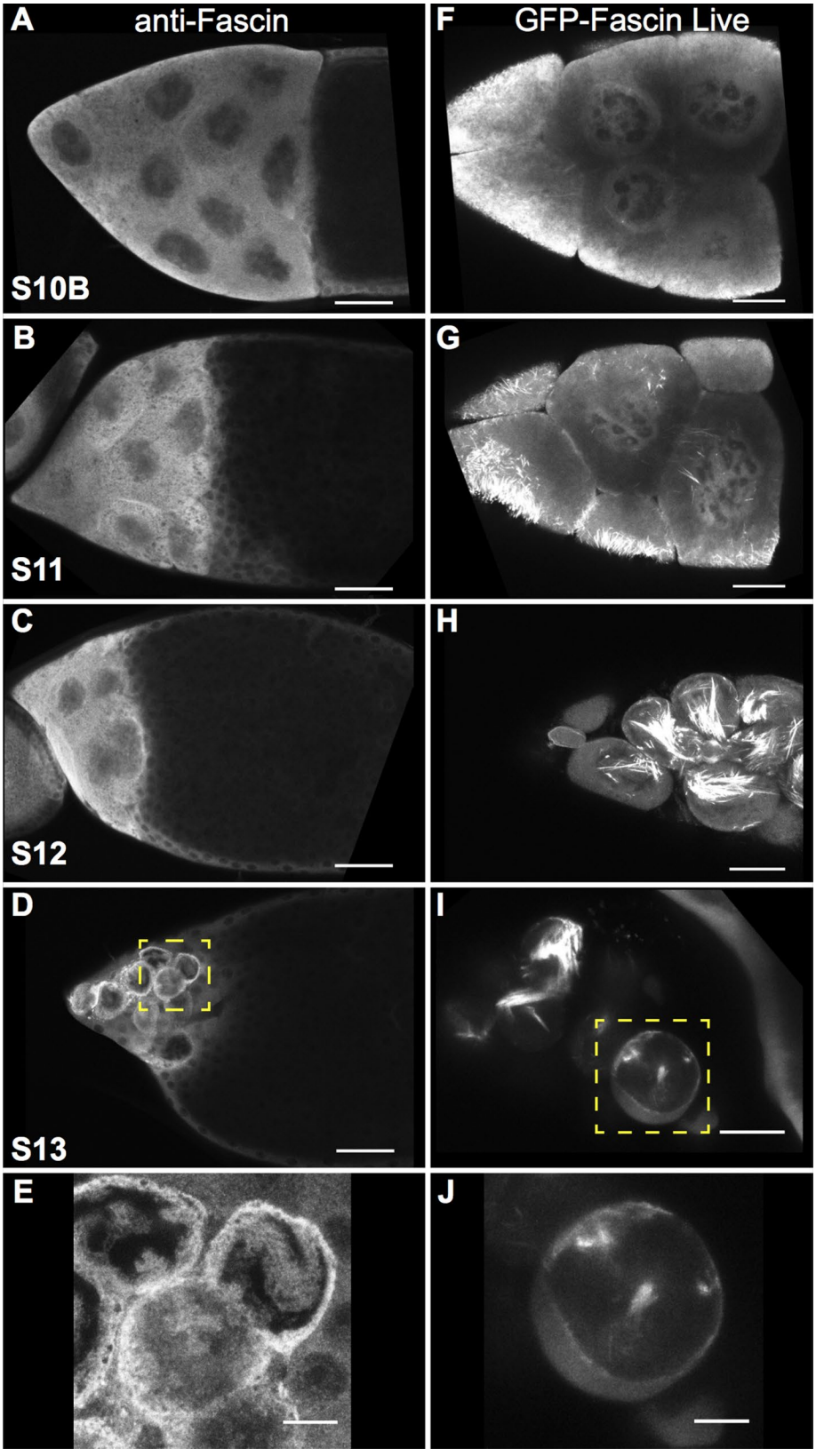

FIGURE 1: Fascin localizes to the nucleus and nuclear periphery during late-stage follicle development. (A–E) Maximum projections of three to five confocal slices of *wild-type* late-stage follicles stained with anti-Fascin. (A) S10B, (B) S11, (C) S12, and (D) S13. (E) Zoomed-in image of yellow boxed region in D. Immunofluorescence analysis of Fascin reveals that Fascin localizes not only to the cytoplasm but also to the nucleus during S10B (A) and that nuclear localization increases during S11 and S12 (B, C). At S13, Fascin relocalizes to the nuclear periphery (D, E). Scale bars, 50 μm (A–D), 10 μm (E). (F–J) Maximum projections of three to five confocal slices showing GFP-Fascin (*UAS GFP Fascin/oskarGal4*) imaged in live follicles using a 40× objective. (F) S10B, (G) S11, (H) S12, and (I) S13. (J) Zoomed-in image of yellow box region in I. Live imaging of late-stage follicles reveals that GFP-Fascin, in addition to being cytoplasmic and on actin bundles, is in the nucleus during S10B–S12 (F–H) and at the nuclear periphery during S13 (I, J). Scale bars, 25 μm (F–I), 10 μm (J).

confocal microscopy. Images revealed that fascin1 was indeed localized at the nuclear envelope and within the nucleus of HeLa carcinoma cells, NIH 3T3 fibroblasts, and THP-1 monocytic-derived cells (Figure 3A), and this staining was specific, as it was not present in fascin1-depleted cells (Figure 3, B and C).

To further confirm the existence of this subcellular distribution, we reexpressed GFP-tagged human fascin1 in fascin1-knockdown HeLa cells fixed and permeabilized with either Triton X-100 or digitonin detergent. Triton permeabilizes both the plasma membrane and the nuclear envelope, whereas digitonin only permeabilizes the plasma membrane (Chang *et al.*, 2013). Therefore comparison of these two permeabilization methods allowed us to assess the specificity of antibody staining inside the nucleus. Triton permeabilization resulted in an enriched fascin1 signal in the perinuclear area and, in a smaller amount, in the nucleus; GFP-fascin1 and anti-GFP antibody signals gave similar intensities throughout (Figure 3, D and E). Cells treated with digitonin showed an absence of lamin staining (due to nonpermeabilized nuclear envelope) coupled with a dramatic decrease of nuclear fascin1 staining (anti-GFP) compared with Triton-treated cells (Figure 3, D and E). Conversely, as expected, the levels of GFP-fascin1 inside the nucleus did not show any difference compared with fully permeabilized cells. Taken together, these results show that a population of fascin1 is localized within the nucleus and in the perinuclear area in a range of mammalian cells, indicating that the localization of Fascin is conserved from *Drosophila* to mammalian cells.

Prostaglandin signaling regulates Fascin localization in *Drosophila*

Because we previously showed that Fascin is a downstream target of PG signaling during S10B of *Drosophila* oogenesis (Groen *et al.*, 2012), we analyzed whether PGs play a role in the localization of Fascin throughout oogenesis. Pxt, the *Drosophila* COX-like enzyme, is required for PG synthesis (Tootle and Spradling, 2008). Two strong

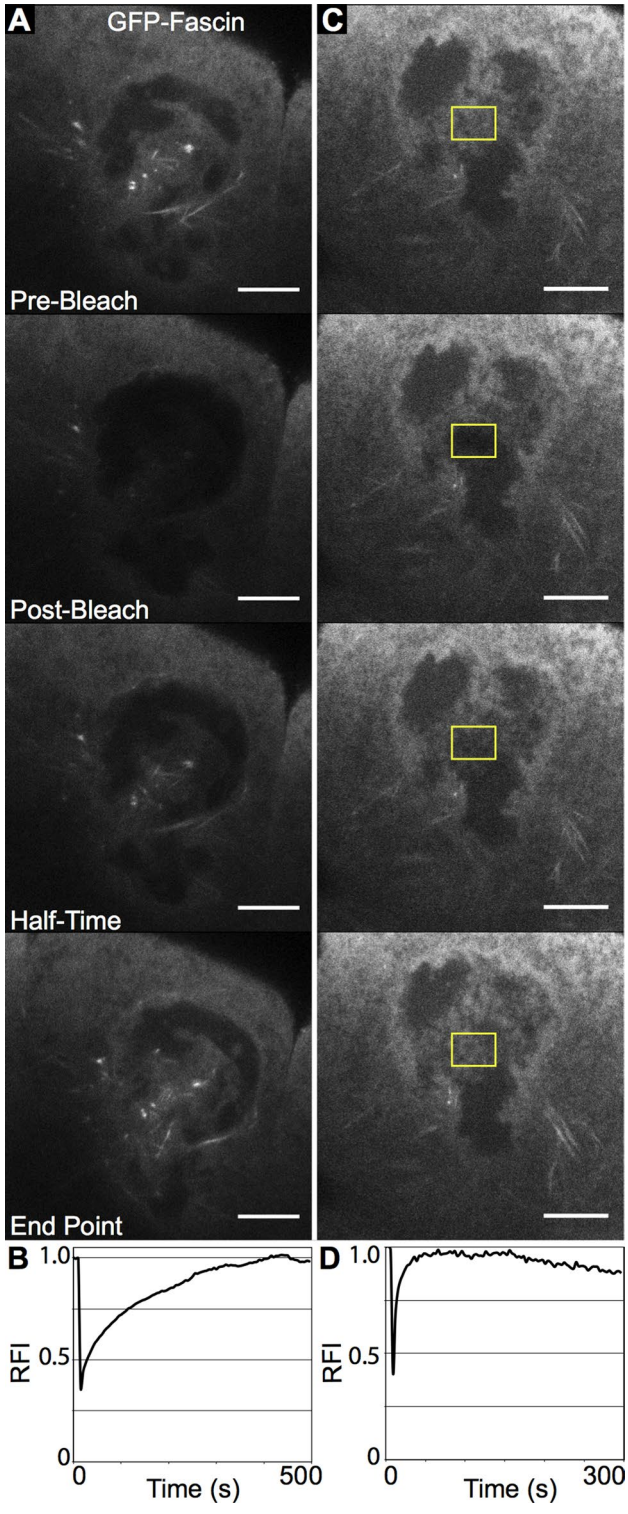

FIGURE 2: GFP-Fascin is dynamic in the nucleus during S10B. (A, C) Representative examples of FRAP experiments. Single-slice confocal images of GFP-Fascin (*UAS GFP Fascin/oskarGal4*) during FRAP time course showing prebleach, postbleach, half of fluorescence intensity recovery, and recovery endpoint. (B, D) Representative FRAP recovery curves plotting relative fluorescence intensity over time. (A, B) Bleach of whole nucleus. FRAP reveals that Fascin is transported into the nucleus during S10B, as fluorescence signal recovers after ~8 min when a whole nucleus is bleached. (C, D) Bleach of small nuclear region (yellow box). Fascin is also dynamic in the nucleus, as a small bleached region recovers fluorescence intensity very rapidly.

loss-of-function alleles of *pxt* were used, termed pxt^{f} and pxt^{EY}. Staining for endogenous Fascin at S10B demonstrated that the relative level of Fascin within the nucleus versus the cytoplasm of *pxt* mutant nurse cells was increased compared with wild type (Supplemental Figure S1, E–E″ compared with A–A″). During S11 and S12, when nuclear Fascin levels are increasing relative the cytoplasm in wild-type follicles, Fascin levels in the nucleus decrease in *pxt* mutants (Supplemental Figure S1, F–G″ compared with B–C″). These *pxt* mutants also exhibit a unique cytoplasmic localization pattern for Fascin immunofluorescence. This "Swiss cheese" appearance is likely due to excess lipid droplet formation in the cytoplasm of *pxt* mutants (unpublished data) and does not reflect a localization change unique to Fascin or a change in total Fascin protein levels (Groen *et al.*, 2012).

To further characterize Fascin localization, we analyzed higher-magnification images of follicles costained for Fascin and wheat-germ agglutinin (WGA), which binds nuclear pore complexes and marks the nuclear envelope. We generated fluorescence intensity plots across nuclei for both Fascin and WGA (yellow arrows in Figure 4, A and B) to precisely analyze Fascin localization. During S10B, in wild-type follicles, Fascin intensity was markedly reduced within the nucleus (between the WGA peaks—marked by black arrows in Figure 4C) compared with the cytoplasm (outside the WGA peak) but above background signal levels. In *pxt* mutants, Fascin intensity was high in the nucleus and increased further in the cytoplasm (Figure 4D). Quantification of multiple intensity plots across posterior nurse cell nuclei confirmed that Fascin levels within the nucleus at S10B were significantly increased in *pxt* mutant compared with wild-type follicles (Figure 4, B and D, compared with A and C and quantified in E). Conversely, nuclear Fascin levels are significantly decreased in *pxt* mutants during S11 and S12 (Figure 4E).

We also performed subcellular fractionation assays on whole-ovary lysates to confirm that Fascin is a nuclear protein and analyze the effects of PGs on Fascin localization. Cytoplasmic and nuclear fractions were analyzed by immunoblot, using Lamin as a nuclear marker and Tubulin as a cytoplasmic marker. Fascin was confirmed in the nuclear fractions (Figure 4F). In addition, quantification of the subcellular fractionation assays revealed that the total amount of nuclear Fascin in *pxt* mutant ovaries was reduced compared with wild type, whereas total Fascin levels are unchanged (Figure 4G). The observation that nuclear Fascin was reduced in *pxt* mutants based on subcellular fractionation likely reflects both the stage-specific alterations in Fascin localization in *pxt* mutants (Supplemental Figure 1, E–G″, and Figure 4E) and a different composition of follicle stages within ovaries (Tootle and Spradling, 2008). Together our data are consistent with the model that PG signaling regulates the subcellular localization of Fascin.

Prostaglandins regulate Fascin localization to the nuclear periphery

During S13, Fascin normally localizes to the nuclear periphery. Intensity plot analysis of wild-type S13 follicles revealed a solitary sharp peak of Fascin fluorescence on each side of the nucleus, with much higher relative fluorescence intensity compared to any other area within the cell. This peak overlapped the WGA peak marking the nuclear envelope (Figure 5, A and C). However, the highest peak Fascin intensity occurred just outside the WGA peak, indicating that Fascin accumulation during S13 is predominantly perinuclear.

Fascin failed to relocalize to the nuclear periphery at S13 in *pxt* mutants (Figure 5B and Supplemental Figure S1, H–I″). In these S13 *pxt* mutant follicles, two distinct localization patterns were observed: Fascin was either absent from the nucleus (Supplemental Figure S1,

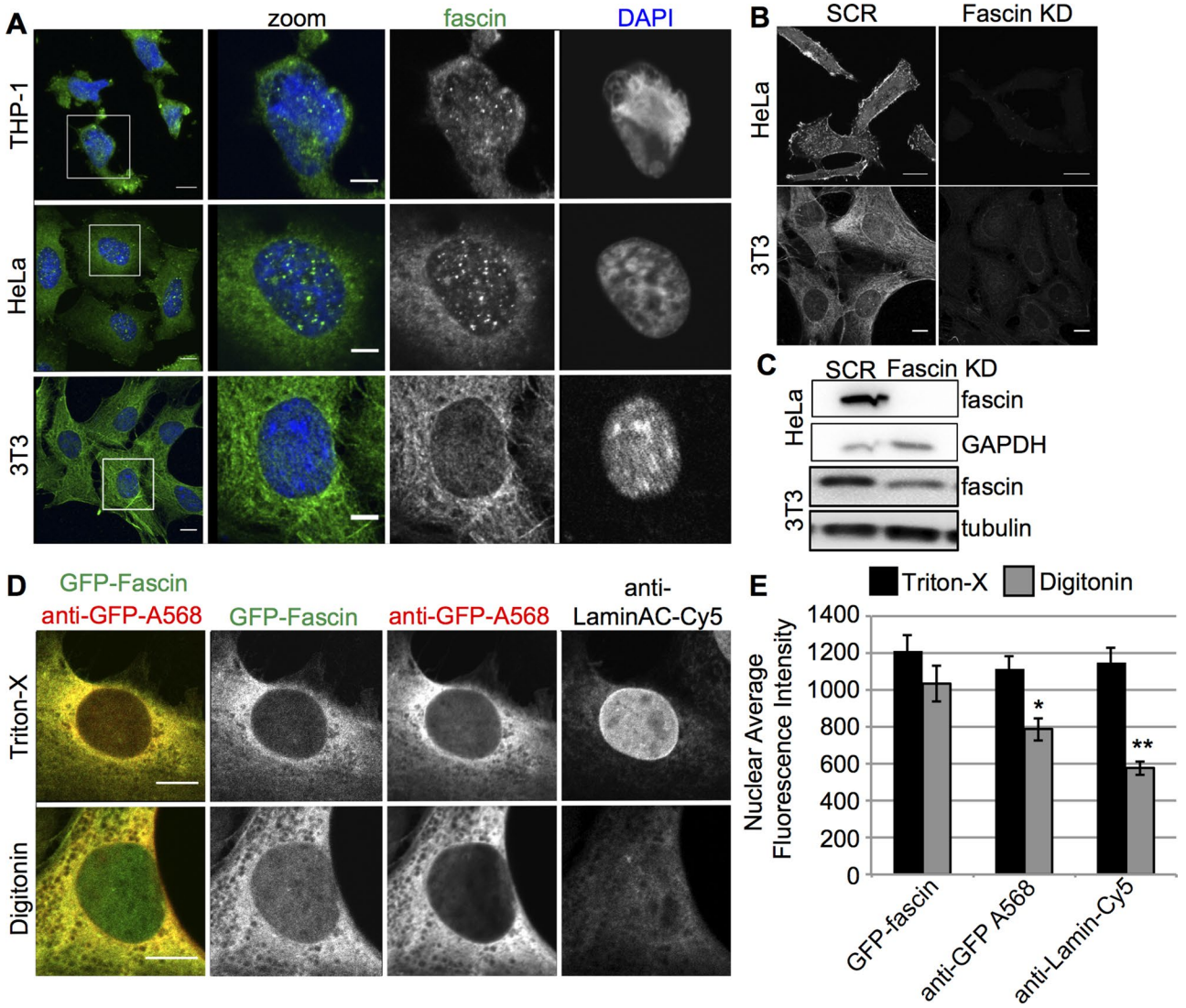

FIGURE 3: Fascin localizes to the nucleus and perinuclear area in a range of mammalian cells. (A) Immunofluorescence of endogenous fascin1 and DNA (DAPI) in THP-1, HeLa, and 3T3 fibroblasts. Left, maximum intensity projections (green, fascin1; blue, DNA); right, single confocal planes of the nuclei highlighted in the white box on the left. Scale bars, 10 μm (left), 5 μm (right). (B) Immunofluorescence for endogenous fascin1 in scrambled (SCR) and fascin1-targetting shRNA (Fascin KD) expressing HeLa and 3T3 fibroblasts. Scale bars. 10 μm. (C) Western blots showing efficient fascin1 KD in cells shown in B. (D) Immunofluorescence of HeLa cells expressing GFP-fascin1, fixed, permeabilized with Triton or digitonin, and stained for fascin1 (Ab-568) and lamin A/C. Left, merged channel image (green, GFP-Fascin; red, anti-GFP). Right, single confocal planes of the indicated channels. (E) Quantification of fascin1 nuclear fluorescence in cells stained as indicated in D. *$p < 0.05$, **$p < 0.01$.

H–H″) or present within the nucleus at a level similar to that observed in the remaining cytoplasm (Supplemental Figure S1, I–I″). Finally, intensity plot analysis confirmed that Fascin does not relocalize to the nuclear periphery at S13 in *pxt* mutants, as Fascin does not exhibit a single sharp peak of fluorescence intensity higher than the surrounding areas (Figure 5D). These data suggest a potential novel PG-dependent and actin-bundling independent role of Fascin at the nuclear periphery.

Nuclear and perinuclear localization is specific to Fascin

During nurse cell dumping, the cytoplasm is rapidly decreasing (S10B–11), and upon its completion, very little cytoplasm remains within the nurse cells (S12–S13). We thus wanted to confirm that our observation of both nuclear and perinuclear Fascin is biologically relevant and not an artifact caused by the drastic reduction of cytoplasmic volume within the nurse cells. To address this, we analyzed the localization of two other actin-binding proteins required for nurse cell dumping, Villin (*Drosophila* Quail, ~97 kDa; Mahajan-Miklos and Cooley, 1994) and Profilin (*Drosophila* Chickadee, ~14 kDa; Cooley *et al.*, 1992). Villin primarily localized to cytoplasmic bundles during S10B (Figure 6, A–B′), whereas Profilin had a more diffuse localization throughout the cytoplasm and nucleus (Supplemental Figure S3, A–B′). This nuclear localization of Profilin is not surprising, as Profilin has been found in numerous systems to enter the nucleus (Stuven *et al.*, 2003; Soderberg *et al.*, 2012). We also analyzed Villin and Profilin localization by subcellular fractionation. A small amount of Villin was present in the nuclear pellet, whereas Profilin was virtually undetectable (Supplemental Figure 3, M and N). This apparent

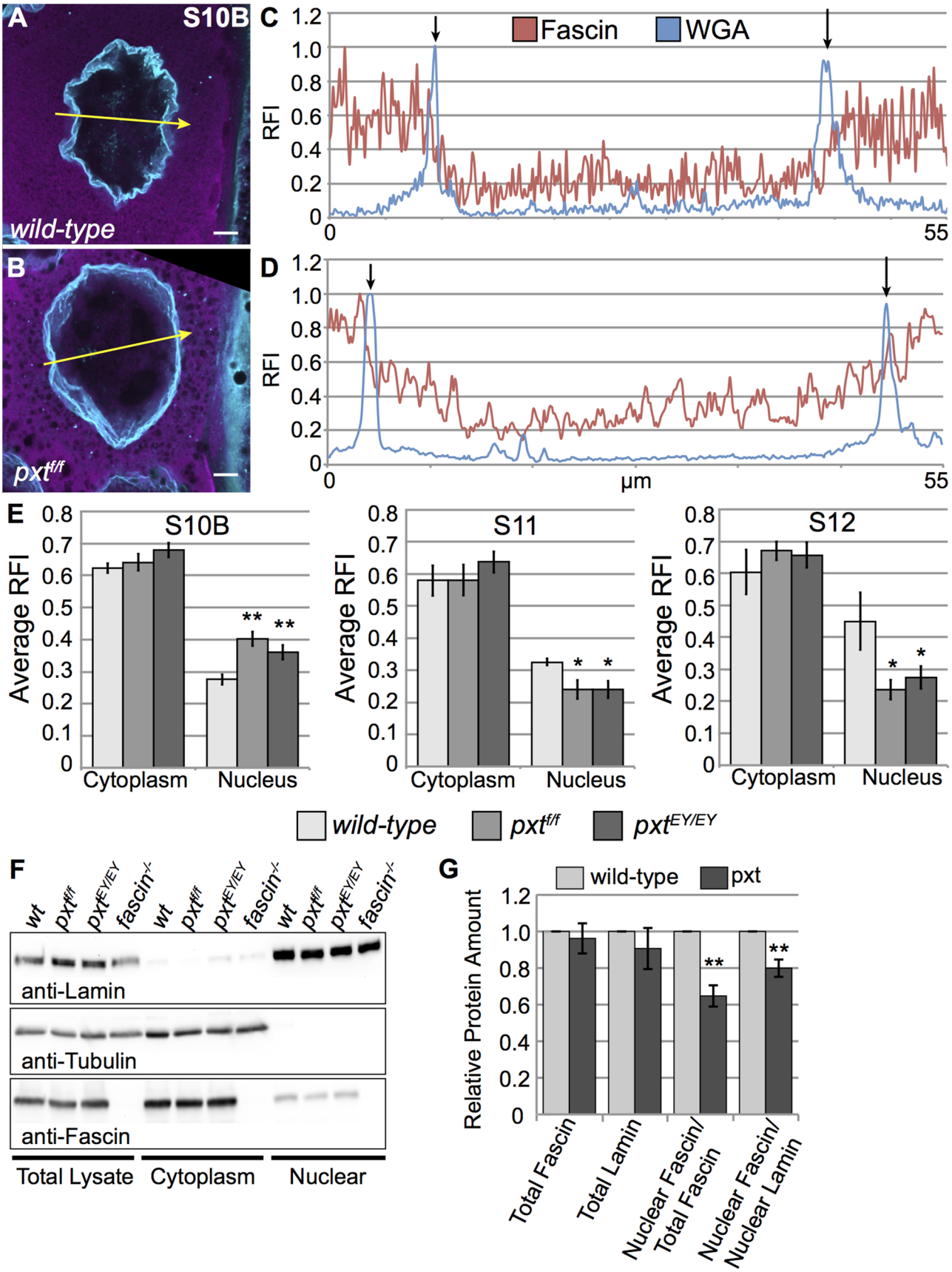

FIGURE 4: Fascin nuclear localization is disrupted in *pxt* mutants. (A, B) Maximum projections of three to five confocal slices of 63× images showing Fascin (magenta) and WGA (nuclear pore complexes, cyan). Scale bars, 10 µm. (A) *wild-type*, (B) *pxt*$^{f/f}$. (C, D) Fluorescence intensity plots of Fascin (red line) and WGA (blue line) along the yellow

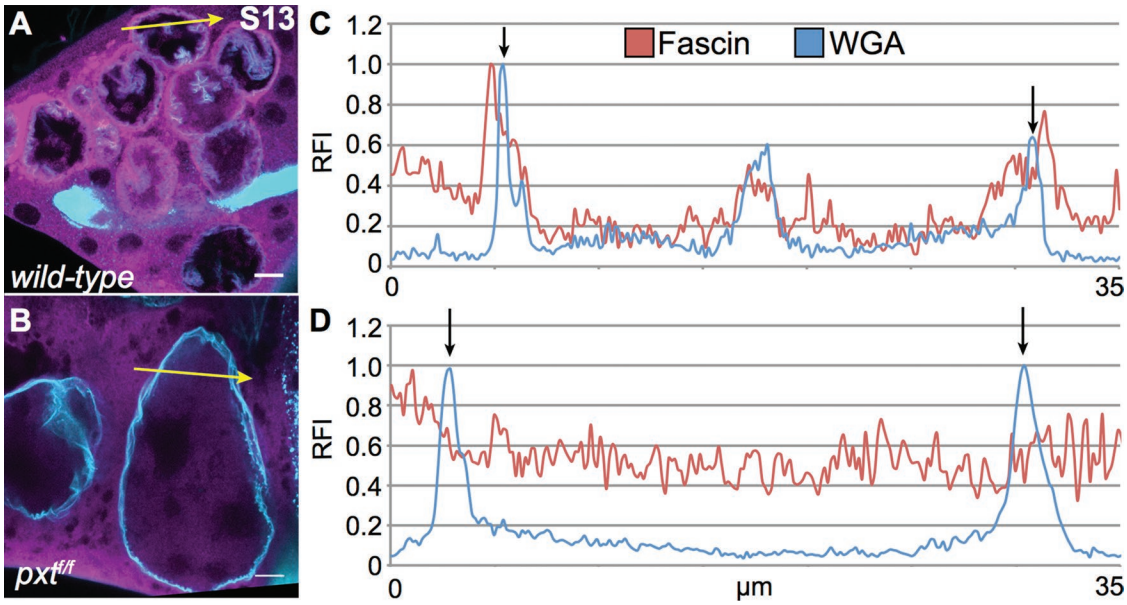

FIGURE 5: Fascin localization to the nuclear periphery during S13 is disrupted in *pxt* mutants. (A, B) Maximum projections of three to five confocal slices of 63× images showing Fascin (magenta) and WGA (nuclear pore complexes, cyan). (A) *wild-type*, (B) $pxt^{f/f}$. (C, D) Fluorescence intensity plots of Fascin (red line) and WGA (blue line) along the yellow arrows in A and B. *x*-axis, distance; *y*-axis, RFI, fluorescence intensity normalized to the brightest point along the plot. Black arrows mark the nuclear envelope (based on WGA peaks). During S13, Fascin localizes to just outside the nuclear envelope (A, C). Loss of PG signaling results in a failure to localize to the nuclear periphery during S13 (B, D).

discrepancy in Profilin localization between the two assays is likely due to the small size of Profilin, which would allow it to freely diffuse out of the nuclei as the follicles are lysed in hypotonic buffer for subcellular fractionation. In summary, these two actin-binding proteins show distinct patterns of localization to the nucleus compared with Fascin.

During S13, both Villin and Profilin localized to the remaining cytoplasmic space of the nurse cells and did not relocalize to the nuclear periphery at S13 (Figure 6, C–D′ and E, and Supplemental Figure 3, C–D′). As an added control, we also used a phosphotyrosine antibody to mark the nurse cell membranes (Supplemental Figure S3, E–H′). This staining pattern is distinct from what is observed with Fascin and shows that both immunofluorescence and fluorescence intensity plots (Supplemental Figure S3, J and L) can distinguish between cell membrane, cytoplasm, and perinuclear localization. Intensity plot analysis on S13 follicles stained for Villin and Profilin confirmed that these proteins do not localize to the nuclear periphery, as the peak intensity is farther away from the nuclear membrane (marked by black arrows) than what is observed with Fascin (Figure 6, E and F, compared with Figure 5, A and C, path marked by yellow arrows, and Supplemental Figure S3K, path marked by yellow arrow in I). To illustrate further the difference in the localization of Villin and Fascin, we quantified the distance of the peak intensity for Villin versus Fascin from the WGA peak using multiple intensity plots. This analysis showed that Villin localized to sites twofold further away from where Fascin localized at the nuclear periphery (Figure 6G). Therefore, the localization of Fascin to the nuclear periphery at S13 is distinct from other actin-binding proteins, suggesting that it likely has a specific and regulated function at this localization.

Nurse cell dumping is required for relocalization of Fascin to the nuclear periphery

Our data demonstrate that nurse cell dumping does not force all actin-binding proteins to the nuclear periphery. However, whether the process of dumping is required for Fascin's relocalization remains unclear. To address this, we analyzed the localization of Fascin in two mutants with defective nurse cell dumping: *villin* and *profilin*. Both of these mutants fail to form elongated cytoplasmic bundles during S10B and thus cannot complete nurse cell dumping (Cooley *et al.*, 1992; Mahajan-Miklos and Cooley, 1994). Fascin localization, both cytoplasmic and nuclear, appears normal during S10B in both of these mutants despite the lack of actin bundles (Supplemental Figure S4,

arrows in A and B. *x*-axis, distance; *y*-axis, RFI, fluorescence intensity normalized to the brightest point along the plot. Black arrows mark the nuclear envelope (based on WGA peaks). (E) Graphs of average RFI (minimum of six intensity plots from at least two images) of Fascin in the nurse cell cytoplasm and nucleus of the follicle stage and genotypes indicated. $^{**}p < 0.01$, $^{*}p < 0.05$ compared with *wild-type* using paired *t* tests, unequal variance. During S10B, Fascin is mainly cytoplasmic but is present at a low level in the nucleus (A, C, E). Loss of PG signaling results in increased nuclear Fascin levels during S10B (B, D, E). During S11 and S12, Fascin levels increase in the nucleus of *wild-type* follicles but decrease in the nuclei of *pxt* mutant follicles (E). (F) Representative Western blot of subcellular fractionation samples (total lysate, cytoplasmic fraction, nuclear fraction) blotted for Lamin Dm0 (nuclear marker), α-Tubulin (cytoplasmic marker), and Fascin. (G) Quantification of Western blots representing five independent subcellular fractionation assays, with protein levels normalized to *wild-type*. Subcellular fractionation assays confirm that Fascin is a nuclear protein (F) and show that in whole ovaries, *pxt* mutants exhibit decreased levels of nuclear Fascin (F, G). $^{**}p < 0.01$ compared with *wild-type* using paired *t* tests, unequal variance.

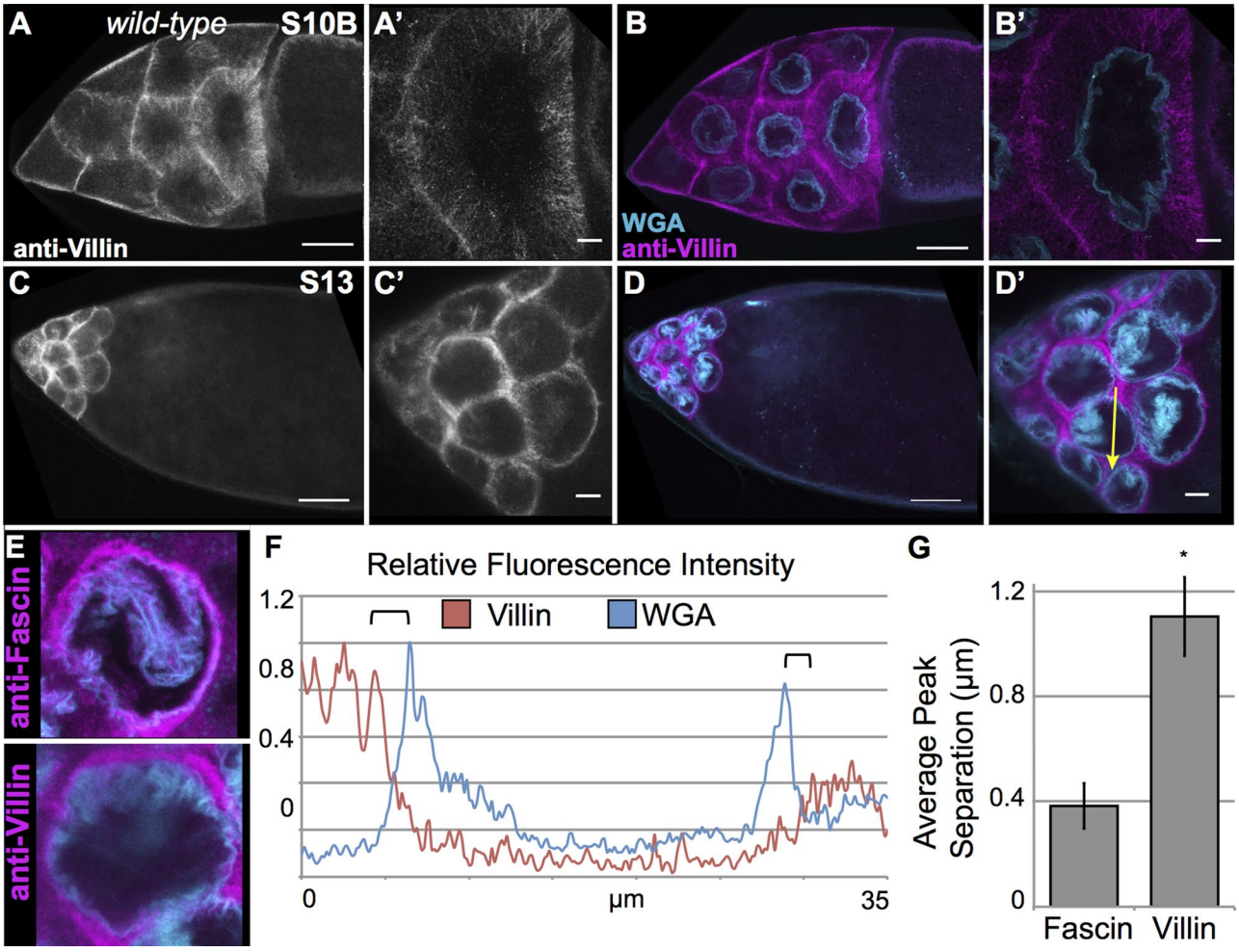

FIGURE 6: Villin has a distinct localization pattern from Fascin. (A–D′) Maximum projections of three to five confocal slices of *wild-type* follicles imaged at 20× (A–D) or 63× (A′–D′). (A, A′, C, C′) Villin (white), (B, B′, D, D′) merged images: Villin (magenta) and WGA (cyan). Villin is primarily present on cytoplasmic actin bundles during S10B and is excluded from the nucleus (A–B′). During S13, Villin is in the remaining cytoplasm and not at the nuclear periphery (C–D′). Scale bars, 50 µm (A–D), 10 µm (A′–D′). (E) Maximum projections of three to five confocal slices of *wild-type* S13 follicles imaged at 63× and cropped to show a single nucleus. Top, follicle stained with anti-Fascin antibody (zoom-in of Figure 5A). Bottom, follicle stained with anti-Villin (zoom-in of D′). (F) Fluorescence intensity plot of Villin (red line) and WGA (blue line) along the yellow arrows in D′. *x*-axis, distance; *y*-axis, RFI, fluorescence intensity normalized to the brightest point along the plot. Black brackets mark the nuclear envelope (based on WGA peaks) and nearest peak cytoplasmic Villin intensity. (G) Graph showing average peak separation between either Fascin or Villin and WGA. Villin localization during S13 is clearly distinct from the perinuclear localization of Fascin. *$p = 0.00029$ compared with *wild-type* using paired *t* tests, unequal variance.

A–B′ and E–F′). However, in S13 mutant follicles (staged by the appearance of dorsal appendages), Fascin failed to relocalize to the nuclear periphery in the majority of observed follicles (Supplemental Figure S4, C–D′ and G–H′). A small percentage (roughly 5–10%) of S13 mutant follicles contained one or two nurse cells that exhibited perinuclear Fascin (unpublished data). The data suggest that the formation of normal cytoplasmic actin bundles is somehow necessary for Fascin localization to the nuclear periphery or that some other aspect of development does not proceed normally in these mutant backgrounds.

Overexpression of GFP-Fascin rescues bundle formation but not perinuclear localization

We previously showed that overexpression of GFP-tagged Fascin in *pxt* mutants rescues the bundle formation and dumping defects due to loss of PGs (Groen *et al.*, 2012). Therefore we expressed GFP-Fascin in a *pxt* mutant background to determine whether Fascin localization is rescued in this context. As shown previously, overexpression of GFP-Fascin rescued cytoplasmic bundle formation, although some bundle defects and cortical actin breakdown are still evident (Supplemental Figure S5, C and C′ compared with A, A′, and E). Consequently, *pxt* mutants expressing GFP-Fascin exhibit increased, but still not complete, nurse cell dumping (Supplemental Figure S5, D and D′ compared with B, B′, and F). Although these follicles dump to a higher degree than *pxt* mutants (Supplemental Figure S5, E–F′), GFP-Fascin still does not localize to the nuclear periphery during S13 in a majority of nurse cells (Supplemental Figure S5, D and D′). These data suggest that nurse cell dumping is not sufficient for perinuclear Fascin relocalization, and in order to relocalize at S13, Fascin must be properly regulated by PG signaling;

alternatively, although GFP-Fascin was previously shown to rescue *fascin*-null mutants (Zanet *et al.*, 2009), it may not be fully able to rescue perinuclear Fascin localization or activity.

Fascin affects nucleolar morphology

The specific, regulated localization of Fascin to the nucleus and nuclear periphery suggests that Fascin has specific functions at these sites. We chose to investigate the potential functions of Fascin within the nucleus. We previously observed a unique nuclear morphology in *fascin* mutant follicles by 4′,6-diamidino-2-phenylindole (DAPI) staining; the DAPI appears fuzzy (unpublished data). We hypothesized that this altered nuclear morphology was due to changes in nucleolar architecture. To test this, we analyzed nucleolar structure by immunofluorescence using an anti-Fibrillarin antibody. Two different null alleles of *fascin* were utilized, termed $fascin^{snX2}$ and $fascin^{sn28}$.

Drosophila nurse cells are very large, polyploid cells expressing high quantities of mRNA, ribosomes, and protein. As such, the nucleolus in these cells is not the circular structure found in diploid cells (Dapples and King, 1970). In *wild-type* follicles, the nurse cell nucleolus is an irregular structure consisting of a series of interconnected tubules (Figure 7, A and A′). Fibrillarin in these *wild-type* follicles localizes within the nucleolar tubules and is most intense along the border of the nucleolus. In *fascin*-null mutants, the nucleolus appears unstructured, as Fibrillarin is dispersed throughout the nucleus (Figure 7, B and B′), lacking the tube-like structure and high-intensity borders of *wild-type* follicles. Because PGs regulate the level of nuclear Fascin (increasing it during S10B but decreasing it globally and during S11–12), we reasoned that if the nucleolar defects observed in *fascin* mutants were due to altered nuclear Fascin levels, then *pxt* mutants should exhibit nucleolar abnormalities. Indeed, we find that in *pxt* mutants, the nucleolus is greatly enlarged with intense Fibrillarin staining at the border and very weak localization on the interior of the nucleolus. Nurse cell nuclei in *pxt* mutants most often exhibit one large circular nucleolus and smaller fragments, in contrast to the multiple interconnected tubules in wild-type nuclei (Figure 7, C and C′ compared with A and A′). Quantification of these phenotypes in two different mutant alleles each for *fascin* and *pxt* shows that 60–80% of *fascin* homozygous mutants have the dispersed phenotype and 40–60% of *pxt* homozygous mutants have an enlarged nucleolar phenotype (Figure 7D). Of interest, heterozygous mutants for either *fascin* or *pxt* trend toward their respective homozygous phenotypes. In addition, when follicle scores are separated by either S10A versus S10B or anterior versus posterior nurse cells, slight variations in the phenotype are evident (Supplemental Tables S1 and S2). The enlarged/fragmented nucleolus in *pxt* mutants is more penetrant in S10B than in S10A follicles. The dispersed phenotype is more prevalent in the four posterior nurse cells than in the anterior nurse cells. This finding suggests that the four posterior nurse cells are unique, an observation made previously (Dapples and King, 1970). Together these data suggest that PG-regulated Fascin affects nucleolar morphology in *Drosophila* nurse cells.

To confirm whether the phenotype we observed was caused by changes in Fascin, we expressed exogenous GFP-tagged Fascin in either *fascin* or *pxt* homozygous mutant background. We observed that overexpression of GFP-Fascin rescues both the dispersed nucleolar phenotype of *fascin* mutants (Figure 7, G and G′ compared with F and F′) and the enlarged/fragmented phenotype of *pxt* mutants (Figure 7, I and I′ compared with H and H′). This finding suggests that the cause of the nucleolar defects in both *fascin* and *pxt* mutants is the loss of nuclear Fascin. Supporting this idea, *pxt* mutants exhibit a global reduction in nuclear Fascin levels observed at the whole-ovary level (Figure 4, F and G).

To assess further the cause of the nucleolar defects in *pxt* and *fascin* mutants, we examined early stages of follicle development to determine when the phenotypes arise. We found that the interconnected tubules shown in *wild-type* S10B follicles (Figure 7, A and A′) are readily observable in S8 and S9 (Figure 8, A and B). The dispersed nucleolar phenotype of *fascin* mutants is also apparent in S8 and S9 of two different alleles, $fascin^{snX2}$ (Figure 8, C and D) and $fascin^{sn28}$ (unpublished data). In *pxt* mutants, enlarged nucleoli are observed in S8 and S9 in the allele termed pxt^{f} (Figure 8, E and F), whereas the other, weaker allele, termed pxt^{EY}, exhibits dispersed nucleoli during S8 and 9 (Figure 8, G and H). These dispersed nucleoli are similar to those observed in *fascin* mutants (Figure 8, C and D). This finding, in conjunction with the pxt^{EY} mutant S10B follicles exhibiting enlarged/fragmented nucleoli (Figure 7D), suggests that the nucleolar phenotypes of *fascin* and *pxt* mutants are similar and likely due to reduction in nuclear Fascin.

One possible reason for the altered nuclear morphology of *pxt* and *fascin* mutants is a lack of normal actin remodeling. The actin bundles formed during S10B in the nurse cells reach the nucleus and cause invaginations in the nuclear envelope (Guild *et al.*, 1997). Thus these bundles could potentially affect nuclear morphology through structures connecting the cytoskeleton to the nucleoskeleton. In the nurses cells, such structures include an actin meshwork (Huelsmann *et al.*, 2013) and may also include the Linker of Nucleoskeleton and Cytoskeleton (LINC) complex (Yu *et al.*, 2006; Technau and Roth, 2008). To address the possibility that loss of normal actin remodeling results in defects in nucleolar structure, we analyzed the nucleolar morphology of two other mutants that lack normal cytoplasmic bundle formation: *profilin* and *villin*. In contrast to the phenotypes observed in *fascin* and *pxt* mutants, *profilin* mutants (Supplemental Figure S6, B and B′) exhibit interconnected tubules similar to wild-type nucleoli (Supplemental Figure S6, A and A′). In *villin* mutants, the nucleoli have an intermediate phenotype, exhibiting properties of both interconnected tubules and mild dispersion (Supplemental Figure S6, C and C′). We speculate that the mild nucleolar alterations in *villin* mutants are due to Fascin having to compensate for the loss of Villin in the cytoplasm, resulting in mild changes in the localization of Fascin. To address this possibility, we reexamined the localization of Fascin in *villin* mutants by immunofluorescence. Although the nuclear localization of Fascin appeared normal in these mutants (Supplemental Figure S4, E–F′), quantification of fluorescence intensity revealed a minor but statistically insignificant decrease in nuclear Fascin fluorescence intensity (Supplemental Figure S6D). In addition, subcellular fractionation of three *villin* transheterozygous mutants revealed a small decrease in nuclear Fascin levels in whole-ovary lysates (Supplemental Figure S6, E and F). Together these data are consistent with the mild nucleolar phenotype of the *villin* mutants and suggest that the phenotypes observed in *pxt* and *fascin* mutants are due to changes in Fascin.

Fascin regulation of nucleolar architecture is conserved in mammalian cells

To define whether Fascin also regulates nucleolar morphology in mammalian cells, we knocked down fascin1 in HeLa cells, stained for Fibrillarin, and carefully analyzed nucleolar phenotypes by confocal microscopy. Quantitative analysis of images revealed that loss of fascin1 results in a small but significant increase in the number of nucleoli and a much stronger increase in total nucleolar area and average nucleolar size (Figure 9, B compared with A and quantified in D). Of importance, reexpression of RFP-fascin1 in the knockdown cells restores the wild-type (scrambled short hairpin RNA [shRNA]) nucleolar number, area, and size (Figure 9, C, quantified in D). These

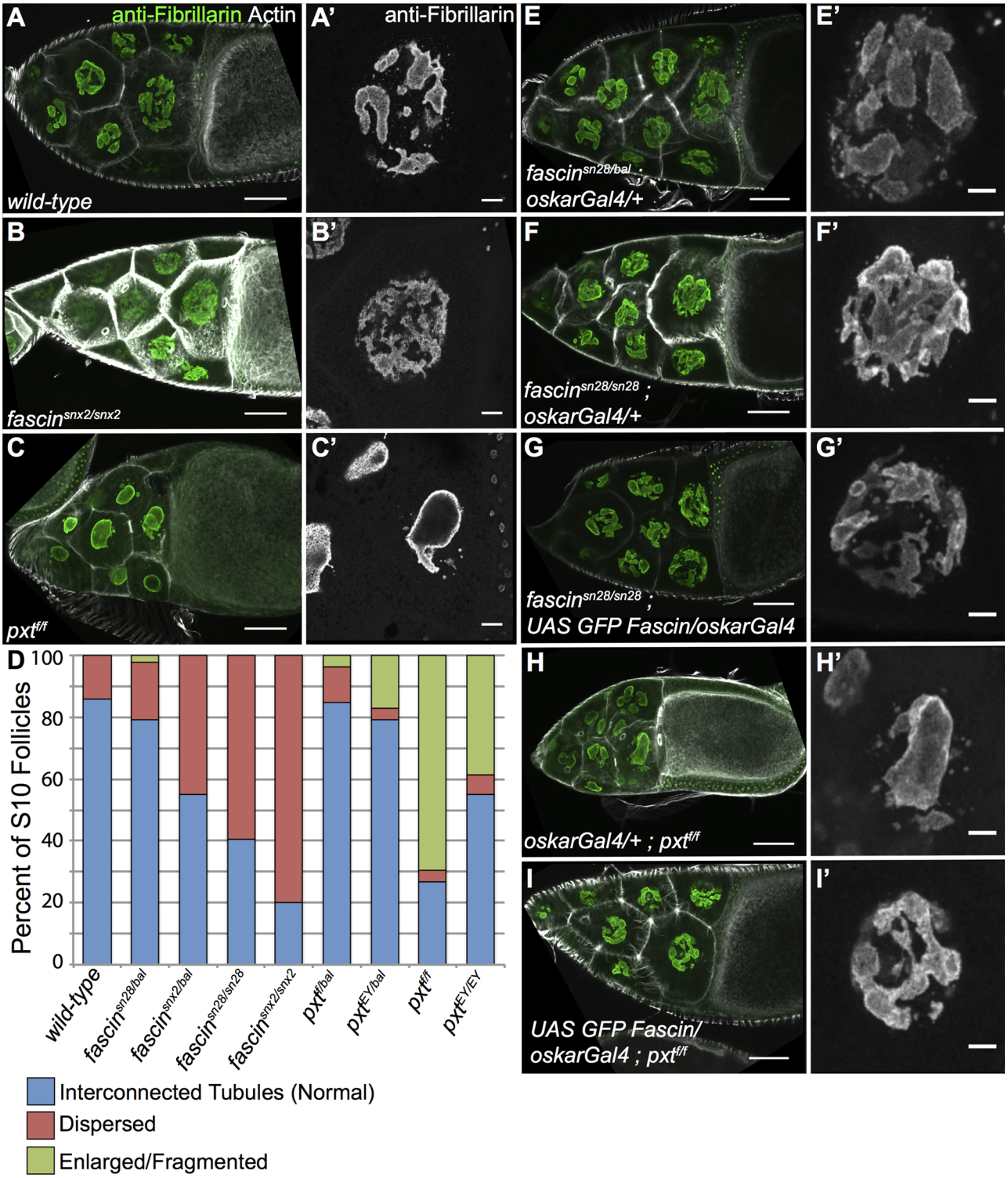

FIGURE 7: Nucleolar structure is altered in *fascin* and *pxt* and mutants. (A–C′, E–I′) Maximum projections of three to five confocal slices at 20× (A–C, E–I) or 63× (A′–C′, E′–I′) of S10B follicles of the indicated genotypes. (A, A′) *wild-type*, (B, B′) *fascin*$^{snx2/snx2}$, (C,C′) *pxt*$^{f/f}$, (E, E′) *fascin*$^{sn28/bal}$; *oskarGal4/+*, (F, F′) *fascin*$^{sn28/sn28}$; *oskarGal4/+*, (G, G′) *fascin*$^{sn28/sn28}$; *UAS GFP Fascin/oskarGal4*, (H, H′) *oskarGal4/+; pxt*$^{f/f}$, and (I, I′) *UAS GFP Fascin/oskarGal4; pxt*$^{f/f}$. (A–C, E–I) Merged images: Fibrillarin (green) and phalloidin (white). (A′–C′, E′–I ′) Fibrillarin (white). (D) Graph showing quantification of nucleolar phenotype in S10 follicles (blue, normal, interconnected tubules; red, dispersed nucleoli; green, enlarged, fragmented nucleoli). Wild-type nucleoli have an interconnected tubule structure (A, A′), whereas *fascin*-mutant nucleoli are dispersed (B, B′) and *pxt*-mutant nucleoli are enlarged and fragmented (C, C′); phenotypic frequencies are quantified in D. Expression of exogenous GFP-Fascin in *fascin*-null mutants (G, G′) rescues the dispersed nucleolar phenotype (F, F′) and more closely resembles the interconnected tubules most often observed in *fascin* heterozygous controls (E, E′). Overexpression of GFP-Fascin in a *pxt* mutant also rescues the enlarged, fragmented nucleoli observed (H, H′ compared with I, I′). Scale bars, 50 μm (A–C, E–I), 10 μm (A′–C′, E′–I′).

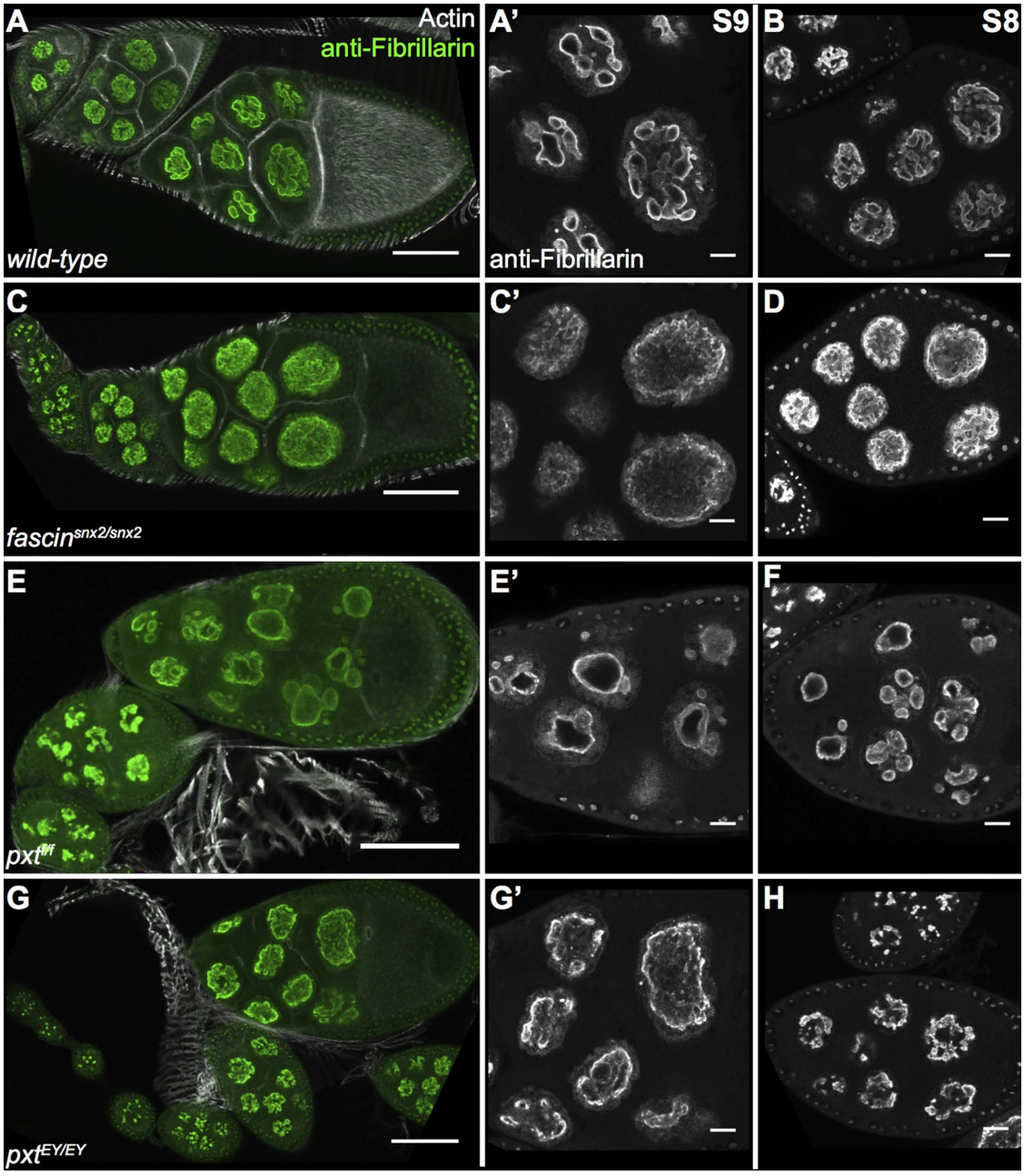

FIGURE 8: Stage 8 and 9 follicles exhibit nucleolar phenotypes. (A–H) Maximum projections of three to five confocal slices at 20× (A, C, E, G) or 63× (A′, B, C′, D, E′, F, G′, H) of follicles of the indicated stages and genotypes. (A, B) *wild-type*, (C, D) *fascin*$^{snx2/snx2}$. (E, F) *pxt*$^{f/f}$, (G, H) *pxt*$^{EY/EY}$. (A, C, E, G) Merged images: Fibrillarin (green) and phalloidin (white). (A′, B, C′, D, E′, F, G′, H) Fibrillarin (white). *Wild-type*, *fascin*-mutant, and *pxt*$^{f/f}$-mutant follicles all display nucleolar phenotypes in stages 8 and 9 that are similar to their respective phenotypes observed during stage 10. However, *pxt*$^{EY/EY}$ mutants have a more dispersed phenotype during S8 and S9 and do not exhibit the enlarged and fragmented nucleoli normally seen in this genotype during S10. Scale bars, 50 μm (A, C, E, G), 10 μm (A′, B, C′, D, E′, F, G′, H).

data strongly indicate that Fascin plays a critical and conserved role in regulating nucleolar architecture.

DISCUSSION

The actin-bundling protein Fascin has long been regarded as a solely cytoplasmic protein with roles in the formation and maintenance of cytoplasmic actin bundle structures, including filopodia (Vignjevic, 2006; Hashimoto *et al.*, 2007) and invadopodia (Li *et al.*, 2010; Schoumacher *et al.*, 2010). Here we provide the first characterization of Fascin as a nuclear protein, showing localization both within the nucleus and proximal to the nuclear envelope in both *Drosophila* and mammalian cell contexts. Of importance, the Fascin antibody we used in the *Drosophila* studies does not recognize Fascin that is bound to F-actin (Cant *et al.*, 1994), suggesting that the localization observed here is independent of the role of Fascin as an F-actin bundler. In addition, we show that the subcellular localization

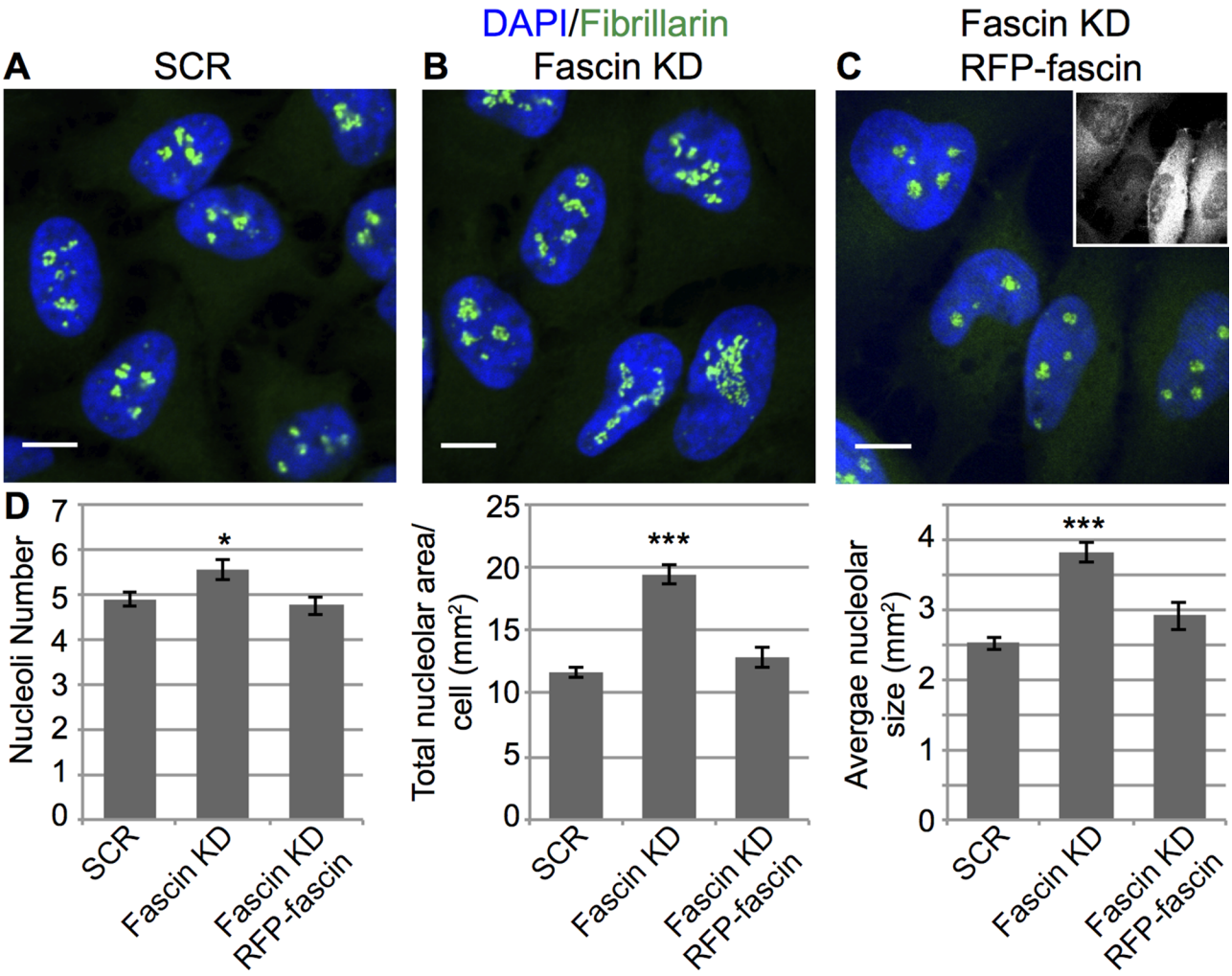

FIGURE 9: Loss of fascin1 affects nucleolar structure in mammalian cells. (A) Immunofluorescence of Fibrillarin (green) and DNA (DAPI, blue) in HeLa cells with scrambled (A), fascin1-targeting shRNA (Fascin KD; B), or fascin1-targeting shRNA with RFP-fascin1 rescue (C). (D) Quantification of nucleolar number, total area, and average size in HeLa cells with the indicated shRNA. Knockdown of fascin1 in HeLa cells leads to an increase in number, total area, and average size of nucleoli, as shown by Fibrillarin staining. *$p < 0.05$, ***$p < 0.001$.

of *Drosophila* Fascin is developmentally dynamic and regulated, as evident by the increase in nuclear Fascin from S10B through S12 and the dramatic relocalization to the nuclear periphery during S13. This localization pattern is perturbed by genetic loss of PG synthesis, suggesting that PG signaling regulates Fascin localization. Although we hypothesize that a specific PG activates a signaling cascade that regulates the localization of Fascin, it is important to note that it remains unknown how direct the regulation of Fascin is by PGs.

We previously showed that Fascin functions as a downstream target of PG signaling to promote actin bundle formation during S10B of *Drosophila* oogenesis (Groen *et al.*, 2012). Our results shown here offer a potential mechanism: PGs regulate Fascin subcellular localization and, thereby, function. We observe increased levels of Fascin within the nucleus during S10B in *pxt* mutant compared with wild-type follicles. This increase of Fascin in the nucleus could contribute to, or be caused by, the decreased formation of actin bundles in *pxt* mutants. We favor the first possibility, as loss of bundle formation in *villin* and *profilin* mutants does not dramatically increase nuclear Fascin levels during S10B. Increased localization of Fascin to the nucleus in *pxt* mutants may therefore result in sequestration of Fascin away from cytoplasmic actin filaments, contributing to the observed loss of actin bundles in these mutants. Indeed, regulators of cytoskeletal remodeling like Rac are sequestered in the nucleus in response to signaling, and this sequestration contributes to modulating the actin cytoskeleton (Navarro-Lerida *et al.*, 2015). Therefore, like other actin-binding proteins, one function of nuclear Fascin localization may be sequestration away from the cytoplasmic actin cytoskeleton.

It seems likely that the roles of Fascin are different within the nucleus and at the nuclear periphery. One possible function of perinuclear Fascin is to serve as part of the complex that links the cytoskeleton to the nucleoplasm and is responsible for nuclear movement and maintenance of nuclear positioning. The LINC complex mediates this function in numerous systems and cell types (reviewed in Rothballer and Kutay, 2013). The LINC complex has also received considerable attention as a key mediator of mammalian cell migration (reviewed in Isermann and Lammerding, 2013). However, the importance of the LINC complex of proteins during *Drosophila* nurse cell dumping has been debated (Yu *et al.*, 2006; Technau and Roth, 2008). Indeed, a recent study identified an actin

meshwork that mediates nurse cell nuclear positioning (Huelsmann *et al.*, 2013). Thus perinuclear Fascin may be a component of the actin meshwork complex in *Drosophila* and may contribute to regulating nuclear shape and architecture in a range of different contexts.

As for the nuclear function of Fascin, we also demonstrated that changes in Fascin at either the expression (*fascin*-null mutants) or localization (*pxt* mutants) level affect nucleolar structure. These effects are not caused by disruption of actin bundle formation, as other bundling-deficient mutants do not exhibit severely altered nucleolar architecture. It remains to be seen whether the altered nucleolar structure in *fascin* and *pxt* mutants affects ribosome production, rRNA transcription, or other mRNA expression. Alternatively, Fascin and Pxt may regulate nonribosomal functions of the nucleolus, such as apoptosis, response to cellular stress, or senescence (reviewed in Boisvert *et al.*, 2007; Ruggero, 2012; Hein *et al.*, 2013). In addition, the observed nucleolar changes may be indicative of a broader role in nuclear organization, including the positioning and/or morphology of other nuclear bodies, such as Cajal bodies (Liu *et al.*, 2006, 2009). Supporting the idea that cytoskeletal regulators that localize to the nucleus play important roles in nuclear organization, it was recently shown that the actin nucleation factor Wash regulates nuclear morphology and chromatin organization (Verboon *et al.*, 2015).

Our finding that the enlarged and fragmented nucleolus in *pxt* mutants is rescued by overexpression of GFP-Fascin suggests the nucleolar defects observed when PGs are lost are due to decreased levels of nuclear Fascin. This idea is consistent with the reduction in nuclear Fascin levels observed at the whole-ovary level in *pxt* mutants. In addition, whereas the nucleolar phenotypes of *fascin* and *pxt* mutants appear distinct during S10B, one allele of *pxt* exhibits a *fascin*-like dispersed nucleolar phenotype during S8–9. Because this *pxt* allele generally exhibits weaker phenotypes than the other allele (Tootle and Spradling, 2008), we postulate that the dispersed nucleolar phenotype is a precursor to the enlarged and fragmented phenotype. This idea suggests that loss of Pxt results in more severe nucleolar defects than loss of Fascin and that PG signaling likely regulates multiple proteins necessary for controlling nucleolar architecture and likely function.

Both PGs and Fascin regulate nucleolar morphology in mammalian systems. It has been shown that pharmacologic inhibition of PG synthesis results in enlarged and misshapen nucleoli and altered protein localization to nucleoli in cultured mammalian cells (Stark *et al.*, 2001; Stark and Dunlop, 2005; Thoms *et al.*, 2007; Khandelwal *et al.*, 2011). Here we show that knockdown of fascin1 in HeLa cells results in a phenotypically similar increase in number, size, and total area of the nucleoli. Future studies are needed to determine the consequences of these nucleolar changes and the extent to which PG regulation of Fascin's nucleolar role is conserved in mammals.

The nucleolus is emerging as a new target for anticancer therapies (reviewed in Ruggero, 2012; Hein *et al.*, 2013; Quin *et al.*, 2014). One of the earliest means pathologists used to distinguish cancer from normal cells was alteration in nucleolar morphology. It was originally believed that the changes in the nucleolus simply reflected its role in protein production. However, recent work suggests that the nucleolus has numerous nonribosomal roles in cell physiology. Proteomic studies reveal that less than half of the nucleolar proteome is related to ribosome biogenesis (Andersen *et al.*, 2002; Scherl *et al.*, 2002; Coute *et al.*, 2006; Leung *et al.*, 2006; Ahmad *et al.*, 2009). Such studies also uncovered that the nucleolar proteome is dynamic and responds the cellular environment (Andersen *et al.*, 2005). This and other work implicate the nucleolus in regulating cell proliferation, differentiation, senescence, and apoptosis and coordinating the cellular response to stress. All of these nucleolar activities could contribute to cancer survival, proliferation, and progression. Indeed, the severity of the changes in nucleolar number and structure is used as a marker of the aggressiveness of the cancer (reviewed in Ruggero, 2012; Hein *et al.*, 2013; Quin *et al.*, 2014). Of note, increased PG production (Rolland *et al.*, 1980; Chen *et al.*, 2001; Khuri *et al.*, 2001; Gallo *et al.*, 2002; Denkert *et al.*, 2003) and up-regulation of fascin1 (Hashimoto *et al.*, 2004; Yoder *et al.*, 2005; Lee *et al.*, 2007; Okada *et al.*, 2007; Li *et al.*, 2008; Chan *et al.*, 2010) are also implicated in tumorigenesis and subsequent metastasis and are associated with highly aggressive cancers and poor patient prognosis. Thus, given our findings, it is tempting to speculate that one of the roles of PG signaling in cancer is to regulate nuclear Fascin levels to modulate nucleolar function.

In summary, we have identified new subcellular sites of Fascin localization—the nucleus and nuclear periphery—in both *Drosophila* and mammalian cells. This conserved, regulated localization suggests that Fascin is likely to have novel activities at these sites, including effects on nucleolar architecture as described here.

MATERIALS AND METHODS

Fly stocks

Fly stocks were maintained on cornmeal/agar/yeast food at 21°C, except where noted. Before immunofluorescence or Western blot analysis, flies were fed wet yeast paste daily for 3 d. Unless otherwise noted, *yw* was used as the wild-type control. The following stocks were obtained from the Bloomington *Drosophila* Stock Center (Bloomington, IN): $pxt^{EY03052}$ (referred to as pxt^{EY}), sn^{34e}, sn^{2}, sn^{x2}, sn^{36a}, $qua^{6\text{-}396}$, $qua^{8\text{-}1062}$, $qua^{EY03072}$, *UASp mRFP-Nup107*, and *matαGal4* (third chromosome). pxt^{f01000}, referred to as pxt^{f}, stock was obtained from the Harvard Exelixis collection (Boston, MA). The *UASp GFP-Fascin* wild-type transgenic fly line was a generous gift from François Payre (Université de Toulouse, Toulouse, France; Zanet *et al.*, 2009), the sn^{28} line was a generous gift from Jennifer Zanet (King's College London, London, United Kingdom; Zanet *et al.*, 2012), $chic^{fs(2)neo1}$ and $chic^{11}$ were generous gifts from Allan Spradling (Carnegie Institution for Science, Baltimore, MD), and the *oskarGal4* (second chromosome) line was a generous gift from Anne Ephrussi (European Molecular Biology Laboratory, Heidelberg, Germany; Telley *et al.*, 2012). Expression of *UASp GFP-Fascin* and/or *UASp mRFP-Nup107* was achieved by crossing to *matαGal4* or *oskarGal4* flies and maintaining fly crosses and progeny at 25°C.

Mammalian cells

Human cervical cancer HeLa cells were from the American Type Culture Collection (Teddington, United Kingdom), and monocytic leukemia–derived THP-1 cells and 3T3 mouse fibroblasts were kind donations from Judy Chen (King's College London, London, United Kingdom) and Gregg Gundersen (Columbia University, New York, NY), respectively. For the generation of SCR and fascin1-knockdown (KD) cells, short hairpin DNAs targeting human fascin1 (5′-GCCTGAAGAAGAAGCAGAT-3′), mouse fascin1 (5′-CGACACAAGAAAGTGTGCCTT-3′), and a scrambled control (5′-GATCGAATAGACCGGACGTAA-3′) were cloned in a pLKO lentiviral vector (RNAi Consortium, Broad Institute, Cambridge, MA) between the *Age*I and *Eco*RI sites. Lentiviral particles were generated, and cells were infected and later selected with puromycin.

Immunofluorescence

Whole-mount *Drosophila* ovary samples were fixed for 10 min at room temperature in 4% paraformaldehyde in Grace's insect

culture medium (Lonza, Walkersville, MD), with the exception of sn 7C–stained ovaries, which were fixed for 15 min in 4% formaldehyde in Grace's medium. Briefly, samples were blocked by washing in Triton antibody wash (1× phosphate-buffered saline [PBS], 0.1% Triton X-100, and 0.1% bovine serum albumin [BSA]) six times for 10 min each. Primary antibodies were incubated overnight at 4°C. Alexa Fluor 647– or rhodamine-conjugated phalloidin (Invitrogen, Life Technologies, Grand Island, NY) was included with both primary and secondary antibodies at a concentration of 1:250. Alexa Fluor 555– or Alexa Fluor 647–conjugated WGA (Invitrogen, Life Technologies) was included with the secondary antibody at a concentration of 1:250 or 1:500. The following primary antibodies were obtained from the Developmental Studies Hybridoma Bank (DSHB) developed under the auspices of the National Institute of Child Health and Human Development and maintained by the Department of Biology, University of Iowa (Iowa City, IA): mouse anti-Fascin 1:25 (sn 7c, Cooley, L.; Cant *et al.*, 1994); mouse anti-Quail 1:50 (6B9, Cooley, L.; Mahajan-Miklos and Cooley, 1994); and mouse anti-Profilin undiluted (chi 1J, Cooley, L.; Verheyen and Cooley, 1994). The following additional antibodies and concentrations were used: rabbit anti-GFP, 1:2500 (Torrey Pines Biolabs, Secaucus, NJ); mouse anti–phosphotyrosine 4G10, 1:500 (Millipore, Billerica, MA); and mouse anti-Fibrillarin 72B9, 1:2.5 (a generous gift from Patrick Dimario, Louisiana State University, Baton Rouge, LA). After six washes in Triton antibody wash (10 min each), secondary antibodies were incubated overnight at 4°C or for 4 h at room temperature. The following secondary antibodies were used at 1:1000: AF488::goat anti-mouse, AF568::goat anti-mouse, and AF488::goat anti-rabbit (Invitrogen, Life Technologies). After six washes in Triton antibody wash (10 min each), DAPI staining was performed at a concentration of 1:10,000 in 1× PBS for 10 min at room temperature. Ovaries were mounted in 1 mg/ml phenylenediamine in 50% glycerol, pH 9 (Platt and Michael, 1983). All experiments were performed a minimum of three independent times.

For immunofluorescence and confocal analysis of fascin1 in mammalian cells, cells were plated onto fibronectin-coated coverslips, fixed with cold 100% methanol for 1 min at –20°C, blocked with bovine serum albumin (BSA; 3%) and stained with anti-fascin1 antibody (DAKO, Cambridge, United Kingdom). For the digitonin permeabilization assays, cells were treated as described in Chang *et al.* (2013). Briefly, cells expressing GFP-fascin1 were fixed with paraformaldehyde (PFA; 4%) and permeabilized with either Triton (0.1%) for 20 min at room temperature or digitonin (0.01%) for 5 min on ice. The cells were blocked with BSA (3%) and stained with anti-GFP (MBL International, Tagoya, Japan) and anti-laminA/C (Abcam, Cambridge, United Kingdom) antibodies. Nucleolar stainings were performed in PFA-fixed cells with the anti–Fibrillarin 72B9 antibody. All Alexa-labeled secondary antibodies were from Life Technologies (Paisley, United Kingdom) and were incubated in BSA (3%). The slides were later mounted using FluorSave (Calbiochem, La Jolla, CA).

Image acquisition and processing

Microscope images of *Drosophila* follicles were obtained using LAS AF SPE Core software on a Leica TCS SPE mounted on a Leica DM2500 using an ACS APO 20×/0.60 IMM CORR -/D or an ACS APO 63×/1.30 Oil CS 0.17/E objective (Leica Microsystems, Buffalo Grove, IL). Maximum projections (three to five confocal slices), merged images, rotation, and cropping were performed using ImageJ software (Abramoff *et al.*, 2004). To aid in visualization, the following panels were brightened by 30% in Photoshop (Adobe, San Jose, CA): Figures 2, A and C, and 6, A–D′, and Supplemental Figures 3, A–H′, I, and J, and 5, A′–D′.

Confocal images of mammalian cells were acquired on a Nikon A1R inverted confocal microscope (Nikon Instruments, Kingston upon Thames, United Kingdom) with a 60× or 100× oil immersion objective. Maximum intensity projections, merged and cropped images, and labeling were performed using ImageJ software.

Live imaging

Whole ovaries were dissected from flies fed wet yeast paste for 3–4 d and maintained at 25°C. Ovaries were dissected in Grace's insect culture media supplemented with 10% fetal bovine serum (Atlanta Biologicals, Flowery Branch, GA) and penicillin/streptomycin (Life Technologies). Late-stage follicles (S10B–S13) were hand dissected and placed in a drop of media on a coverslip-bottom dish (MatTek, Ashland, MA). Live imaging of GFP-Fascin and mRFP-Nup107 was performed using Zen software on a Zeiss 700 LSM mounted on an Axio Observer.Z1 using an LD C-APO 40×/1.1 W/0 objective (Carl Zeiss Microscopy, Thornwood, NY). For FRAP experiments, GFP-Fascin was photobleached using 100% laser power of the 488- nm laser for 50 iterations. One hundred images were obtained in a time series (3 prebleach and 97 postbleach) with no delay between images. FRAP recovery curve analysis was performed using the FRAP Calculator Macro plug-in in ImageJ (Abramoff *et al.*, 2004) on 18 individual nuclei from 15 follicles for whole nucleus bleach and on 8 individual nuclei from 8 follicles for partial nucleus bleach.

Immunofluorescence intensity plots

Fluorescence intensity plots of nurse cell nuclei were generated from a single slice of 63× confocal images using ImageJ software (Abramoff *et al.*, 2004). Briefly, the image background was subtracted using ImageJ (50-pixel rolling ball radius), and then a line segment was drawn across one of the four posterior nurse cell nuclei nearest the oocyte, and the plot profile function was used to generate a fluorescence intensity plot for each desired channel. The raw data files generated by these plot profiles were analyzed in Excel (Microsoft, Redmond, WA), with each plot line normalized to the peak value within that plot, creating intensity plots where the maximum observed fluorescence of a given line is represented by a value of 1.0 relative fluorescence intensity (RFI). The nuclear envelope was marked as the set of data points in which the WGA value was at least 0.5. All RFI averaging was performed in Excel. The cytoplasm was defined as all plot points to the left of the first identified WGA peak and to the right of the second WGA peak (excluding those points that constitute the nuclear membrane peak itself, WGA RFI > 0.5). The nuclear region was defined as all plot points between the two WGA peaks (excluding the nuclear membrane). The distance from the nucleus was defined by first identifying the *x*-coordinate with the highest WGA intensity (WGA peak). The nearest cytoplasmic peak of fluorescence intensity of the protein of interest (Fascin or Villin) was then identified, and the *x*-coordinate with the highest intensity was marked as the peak. The average peak separation was then determined using these *x*-coordinates. A minimum of six nuclei from at least two separate follicles/images were analyzed per genotype for S10B analysis. A minimum of nine nuclei from three separate follicles/images were analyzed per genotype for S13 analysis. Statistical significance was determined used paired Student's *t* tests, unequal variance, in Excel. Fluorescence intensity plots of confocal images of mammalian cells were similarly analyzed using ImageJ. Nuclear area was segmented using DAPI channel, and the average fluorescence intensity for the different channels within nuclear regions was measured from at least 30 cells.

Quantification of nucleolar morphology

Quantification of nucleolar morphology was performed on follicles stained with anti-Fibrillarin antibody, phalloidin (F-actin), and DAPI (DNA). Samples were analyzed using a Leica TCS SPE mounted on a Leica DM2500 using an ACS APO 20×/0.60 IMM CORR -/D objective. All stage 10 follicles on a slide were scored for staging (S10A or S10B) based on follicle size, nurse cell:oocyte ratio, presence of cytoplasmic actin bundles, and migration of border cells and centripetal cells using the DAPI and phalloidin channels. Eleven anterior nurse cells and the four posterior nurse cells (adjacent to the oocyte) were then separately scored for nucleolar morphology (interconnected tubules, enlarged, or dispersed) based on Fibrillarin staining. Scoring was performed by observation through the oculars, and a single slice confocal image was obtained for fibrillarin for each scored follicle. A minimum of 25 follicles from four separate experiments were scored for each genotype.

In mammalian cells, quantification of nucleolar morphology was performed on confocal images of HeLa cells stained with anti-Fibrillarin antibody and DAPI (DNA). A macro was generated in ImageJ to segment the nuclear area using the DAPI signal and quantify nucleolar number, total nucleolar area, and size based on the Fibrillarin staining. A minimum of 96 cells were analyzed per condition.

Western blotting

Western blots were performed using standard methods with the following primary antibodies obtained from the DSHB: mouse anti-Fascin (sn 7C, Cooley, L.) 1:20; mouse anti-Quail (6B9, Cooley, L.) 1:50; rat anti-Vasa (Spradling, A.C., and Williams, D.); 1:100; mouse anti-Lamin Dm0 (ADL195, Fisher, P.A.) 1:200; mouse anti-Profilin (chi 1J, Cooley, L.) 1:10. Mouse anti–α-Tubulin T9026 (Sigma-Aldrich, St. Louis, MO) was used at 1:1000. All blots had 0.1% Tween 20 added to the primary antibody in 5% milk diluted in 1× Tris-buffered saline. The following secondary antibodies were used: peroxidase-AffiniPure goat anti-rat immunoglobulin (IgG; H+L; 1:5000) or peroxidase-AffiniPure goat anti-mouse IgG (H+L; 1:5000; Jackson ImmunoResearch Laboratories, West Grove, PA). Blots were developed with SuperSignal West Pico Chemiluminescent Substrate (Thermo Scientific, Waltham, MA) and imaged using ChemiDoc-It Imaging System and VisionWorksLS software (UVP, Upland, CA). Bands were quantified using the gel analyzer function of ImageJ (Abramoff *et al.*, 2004). A minimum of three independent experiments were performed for each Western blotting experiment.

For mammalian cells experiments, anti-fascin1 antibody (DAKO), anti–β-tubulin (Sigma-Aldrich, Dorset, United Kingdom), and anti–glyceraldehyde-3-phosphate dehydrogenase (Source Bioscience, Nottingham, United Kingdom) were used at 1:1000, 1:5000, and 1:10,000 dilution, respectively, in 5% milk diluted in 1× Tris-buffered saline and 0.1% Tween. Horseradish peroxidase–conjugated polyclonal anti-mouse immunoglobulins (DAKO) were used for secondary antibody detection.

Subcellular fractionation

Subcellular fractionation was performed using methods modified from Guilluy *et al.* (2011). In short, whole ovaries from adult females that had been reared on wet yeast paste for 3–5 d were dissected in room temperature Grace's insect medium (Lonza). Ovaries were lysed in 1.5-ml microcentrifuge tubes on ice in 100 µl of hypotonic buffer (10 mM 4-(2-hydroxyethyl)-1-piperazineethanesulfonic acid, pH 7.9, 1.5 $MgCl_2$, 10 mM KCl, 0.5 mM dithiothreitol, 20 µg/ml aprotinin, 1 mM phenylmethylsulfonyl fluoride) with gentle grinding with a plastic pestle. A rough nuclear pellet was separated from the cytoplasmic fraction by centrifugation at 300 × *g* for 10 min at 4°C (Centrifuge 5415R; Eppendorf, Hauppauge, NY). The nuclear pellet was further clarified using a 25% iodixanol gradient (OptiPrep 60% iodixanol solution diluted with 0.25 M sucrose, 25 mM KCl, 5 mM $MgCl_2$, 20 mM Tris-Cl, pH 7.8). Specifically, the nuclear pellet was resuspended in iodixanol and centrifuged at 10,000 × *g* for 10 min at 4°C. Iodixanol supernatant was removed and the step repeated one time before resuspension of the nuclear pellet in 50 mM Tris-HCl, pH 7.6, 500 mM NaCl, 1% Triton X-100, 0.1% SDS, and 10 mM $MgCl_2$. Equivalent volumes of protein lysates for total cell lysate, cytoplasmic fraction, and nuclear fraction were analyzed by SDS–PAGE/Western blot analysis using the following primary antibodies: mouse anti-Fascin (sn 7C; Cooley, L., DSHB) 1:20; mouse anti-Lamin Dm0 (ADL195, Fisher, P.A., DSHB, 1:200; and mouse anti–α-Tubulin (Sigma-Aldrich) 1:1000; mouse anti-Quail (6B9, Cooley, L.) 1:50; and mouse anti-Profilin (chi 1J, Cooley, L.) 1:10. A minimum of three independent experiments were performed for each subcellular fractionation experiment.

ACKNOWLEDGMENTS

We thank the Lin, Frank, Stipp, Dupuy, and Henry labs for helpful discussions and members of the Tootle lab for helpful discussions and careful review of the manuscript. Data storage support was provided by the Institute for Clinical and Translational Science, which is funded through the Clinical and Translational Science Award supported by the National Center for Research Resources and the National Center for Advancing Translational Sciences, National Institutes of Health, through Grant UL1RR024979. This project is supported by Grant MCB-1158527 from the National Science Foundation, a Carver Trust Medical Research Initiative Grant, and the Medical Research Council (United Kingdom) through MR/J000647/1.

REFERENCES

Abramoff MD, Magalhaes PJ, Ram SJ (2004). Image processing with ImageJ. Biophotonics Int 11, 36–42.

Ahmad Y, Boisvert FM, Gregor P, Cobley A, Lamond AI (2009). NOPdb: Nucleolar Proteome Database—2008 update. Nucleic Acids Res 37, D181–184.

Andersen JS, Lam YW, Leung AK, Ong SE, Lyon CE, Lamond AI, Mann M (2005). Nucleolar proteome dynamics. Nature 433, 77–83.

Andersen JS, Lyon CE, Fox AH, Leung AK, Lam YW, Steen H, Mann M, Lamond AI (2002). Directed proteomic analysis of the human nucleolus. Curr Biol 12, 1–11.

Anilkumar N, Parsons M, Monk R, Ng T, Adams JC (2003). Interaction of fascin and protein kinase Cα: a novel intersection in cell adhesion and motility. EMBO J 22, 5390–5402.

Birukova AA, Zagranichnaya T, Fu P, Alekseeva E, Chen W, Jacobson JR, Birukov KG (2007). Prostaglandins PGE2 and PGI2 promote endothelial barrier enhancement via PKA- and Epac1/Rap1-dependent Rac activation. Exp Cell Res 313, 2504–2520.

Boisvert FM, van Koningsbruggen S, Navascues J, Lamond AI (2007). The multifunctional nucleolus. Nat Rev Mol Cell Biol 8, 574–585.

Bulin C, Albrecht U, Bode JG, Weber AA, Schror K, Levkau B, Fischer JW (2005). Differential effects of vasodilatory prostaglandins on focal adhesions, cytoskeletal architecture, and migration in human aortic smooth muscle cells. Arterioscler Thromb Vasc Biol 25, 84–89.

Cant K, Cooley L (1996). Single amino acid mutations in Drosophila fascin disrupt actin bundling function in vivo. Genetics 143, 249–258.

Cant K, Knowles BA, Mooseker MS, Cooley L (1994). Drosophila Singed, a fascin homolog, is required for actin bundle formation during oogenesis and bristle extension. J Cell Biol 125, 369–380.

Chan C, Jankova L, Fung CL, Clarke C, Robertson G, Chapuis PH, Bokey L, Lin BP, Dent OF, Clarke S (2010). Fascin expression predicts survival after potentially curative resection of node-positive colon cancer. Am J Surg Pathol 34, 656–666.

Chang W, Folker ES, Worman HJ, Gundersen GG (2013). Emerin organizes actin flow for nuclear movement and centrosome orientation in migrating fibroblasts. Mol Biol Cell 24, 3869–3880.

Chen WS, Wei SJ, Liu JM, Hsiao M, Kou-Lin J, Yang WK (2001). Tumor invasiveness and liver metastasis of colon cancer cells correlated with cyclooxygenase-2 (COX-2) expression and inhibited by a COX-2-selective inhibitor, etodolac. Int J Cancer 91, 894–899.

Cooley L, Verheyen E, Ayers K (1992). chickadee encodes a profilin required for intercellular cytoplasm transport during Drosophila oogenesis. Cell 69, 173–184.

Coute Y, Burgess JA, Diaz JJ, Chichester C, Lisacek F, Greco A, Sanchez JC (2006). Deciphering the human nucleolar proteome. Mass Spectrom Rev 25, 215–234.

Dapples C, King R (1970). The development of the nucleolus of the ovarian nurse cell of Drosophila melanogaster. Z Zellforsch 103, 34–47.

Denkert C, Winzer KJ, Muller BM, Weichert W, Pest S, Kobel M, Kristiansen G, Reles A, Siegert A, Guski H, Hauptmann S (2003). Elevated expression of cyclooxygenase-2 is a negative prognostic factor for disease free survival and overall survival in patients with breast carcinoma. Cancer 97, 2978–2987.

Dormond O, Bezzi M, Mariotti A, Ruegg C (2002). Prostaglandin E2 promotes integrin alpha Vbeta 3-dependent endothelial cell adhesion, rac-activation, and spreading through cAMP/PKA-dependent signaling. J Biol Chem 277, 45838–45846.

Edwards RA, Bryan J (1995). Fascins, a family of actin bundling proteins. Cell Motil Cytoskeleton 32, 1–9.

Elkhatib N, Neu MB, Zensen C, Schmoller KM, Louvard D, Bausch AR, Betz T, Vignjevic DM (2014). Fascin plays a role in stress fiber organization and focal adhesion disassembly. Curr Biol 24, 1492–1499.

Funk CD (2001). Prostaglandins and leukotrienes: advances in eicosanoid biology. Science 294, 1871–1875.

Gallo O, Masini E, Bianchi B, Bruschini L, Paglierani M, Franchi A (2002). Prognostic significance of cyclooxygenase-2 pathway and angiogenesis in head and neck squamous cell carcinoma. Hum Pathol 33, 708–714.

Groen CM, Spracklen AJ, Fagan TN, Tootle TL (2012). Drosophila Fascin is a novel downstream target of prostaglandin signaling during actin remodeling. Mol Biol Cell 23, 4567–4578.

Guild GM, Connelly PS, Shaw MK, Tilney LG (1997). Actin filament cables in *Drosophila* nurse cells are composed of modules that slide passively past one another during dumping. J Cell Biol 138, 783–797.

Guilluy C, Dubash AD, García-Mata R (2011). Analysis of RhoA and Rho GEF activity in whole cells and the cell nucleus. Nat Protocols 6, 2050–2060.

Hashimoto Y, Parsons M, Adams JC (2007). Dual actin-bundling and protein kinase C-binding activities of fascin regulate carcinoma cell migration downstream of Rac and contribute to metastasis. Mol Biol Cell 18, 4591–4602.

Hashimoto Y, Shimada Y, Kawamura J, Yamasaki S, Imamura M (2004). The prognostic relevance of fascin expression in human gastric carcinoma. Oncology 67, 262–270.

Hashimoto Y, Skacel M, Adams JC (2005). Roles of fascin in human carcinoma motility and signaling: prospects for a novel biomarker? Int J Biochem Cell Biol 37, 1787–1804.

Hein N, Hannan KM, George AJ, Sanij E, Hannan RD (2013). The nucleolus: an emerging target for cancer therapy. Trends Mol Med 19, 643–654.

Hudson AM, Cooley L (2002). Understanding the function of actin-binding proteins through genetic analysis of Drosophila oogenesis. Annu Rev Genet 36, 455–488.

Huelsmann S, Ylanne J, Brown NH (2013). Filopodia-like actin cables position nuclei in association with perinuclear actin in Drosophila nurse cells. Dev Cell 26, 604–615.

Isermann P, Lammerding J (2013). Nuclear mechanics and mechanotransduction in health and disease. Curr Biol 23, R1113–R1121.

Jaiswal R, Breitsprecher D, Collins A, Corrêa, Ivan R, Xu M-Q, Goode Bruce L (2013). The formin Daam1 and fascin directly collaborate to promote filopodia formation. Curr Biol 23, 1373–1379.

Jayo A, Parsons M, Adams JC (2012). A novel Rho-dependent pathway that drives interaction of fascin-1 with p-Lin-11/Isl-1/Mec-3 kinase (LIMK) 1/2 to promote fascin-1/actin binding and filopodia stability. BMC Biol 10, 72.

Keminer O, Peters R (1999). Permeability of single nuclear pores. Biophys J 77, 217–228.

Khandelwal N, Simpson J, Taylor G, Rafique S, Whitehouse A, Hiscox J, Stark LA (2011). Nucleolar NF-kappaB/RelA mediates apoptosis by causing cytoplasmic relocalization of nucleophosmin. Cell Death Differ 18, 1889–1903.

Khuri FR, Wu H, Lee JJ, Kemp BL, Lotan R, Lippman SM, Feng L, Hong WK, Xu XC (2001). Cyclooxygenase-2 overexpression is a marker of poor prognosis in stage I non-small cell lung cancer. Clin Cancer Res 7, 861–867.

Lee TK, Poon RT, Man K, Guan XY, Ma S, Liu XB, Myers JN, Yuen AP (2007). Fascin over-expression is associated with aggressiveness of oral squamous cell carcinoma. Cancer Lett 254, 308–315.

Leung AK, Trinkle-Mulcahy L, Lam YW, Andersen JS, Mann M, Lamond AI (2006). NOPdb: Nucleolar Proteome Database. Nucleic Acids Res 34, D218–D220.

Li A, Dawson JC, Forero-Vargas M, Spence HJ, Yu X, König I, Anderson K, Machesky LM (2010). The actin-bundling protein fascin stabilizes actin in invadopodia and potentiates protrusive invasion. Curr Biol 20, 339–345.

Li X, Zheng H, Hara T, Takahashi H, Masuda S, Wang Z, Yang X, Guan Y, Takano Y (2008). Aberrant expression of cortactin and fascin are effective markers for pathogenesis, invasion, metastasis and prognosis of gastric carcinomas. Int J Oncol 33, 69–79.

Liu JL, Murphy C, Buszczak M, Clatterbuck S, Goodman R, Gall JG (2006). The *Drosophila melanogaster* Cajal body. J Cell Biol 172, 875–884.

Liu JL, Wu Z, Nizami Z, Deryusheva S, Rajendra TK, Beumer KJ, Gao H, Matera AG, Carroll D, Gall JG (2009). Coilin is essential for Cajal body organization in Drosophila melanogaster. Mol Biol Cell 20, 1661–1670.

Mahajan-Miklos S, Cooley L (1994). The villin-like protein encoded by the Drosophila *quail* gene is required for actin bundle assembly during oogenesis. Cell 78, 291–301.

Navarro-Lerida I, Pellinen T, Sanchez SA, Guadamillas MC, Wang Y, Mirtti T, Calvo E, Del Pozo MA (2015). Rac1 nucleocytoplasmic shuttling drives nuclear shape changes and tumor invasion. Dev Cell 32, 318–334.

Okada K, Shimura T, Asakawa K, Hashimoto S, Mochida Y, Suehiro T, Kuwano H (2007). Fascin expression is correlated with tumor progression of extrahepatic bile duct cancer. Hepato-gastroenterology 54, 17–21.

Peppelenbosch MP, Tertoolen LGJ, Hage WJ, de Laat SW (1993). Epidermal growth factor-induced actin remodeling is regulated by 5-lipoxygenase and cyclooxygenase products. Cell 74, 565–575.

Pierce KL (1999). Activation of FP prostanoid receptor isoforms leads to Rho-mediated changes in cell morphology and in the cell cytoskeleton. J Biol Chem 274, 35944–35949.

Platt JL, Michael AF (1983). Retardation of fading and enhancement of intensity of immunofluorescence by p-phenylenediamine. J Histochem Cytochem 31, 840–842.

Quin JE, Devlin JR, Cameron D, Hannan KM, Pearson RB, Hannan RD (2014). Targeting the nucleolus for cancer intervention. Biochim Biophys Acta 1842, 802–816.

Rolland PH, Martin PM, Jacquemier J, Rolland AM, Toga M (1980). Prostaglandin in human breast cancer: evidence suggesting that an elevated prostaglandin production is a marker of high metastatic potential for neoplastic cells. J Nat Cancer Inst 64, 1061–1070.

Rothballer A, Kutay U (2013). The diverse functional LINCs of the nuclear envelope to the cytoskeleton and chromatin. Chromosoma 122, 415–429.

Ruggero D (2012). Revisiting the nucleolus: from marker to dynamic integrator of cancer signaling. Sci Signal 5, pe38.

Scherl A, Coute Y, Deon C, Calle A, Kindbeiter K, Sanchez JC, Greco A, Hochstrasser D, Diaz JJ (2002). Functional proteomic analysis of human nucleolus. Mol Biol Cell 13, 4100–4109.

Schoumacher M, Goldman RD, Louvard D, Vignjevic DM (2010). Actin, microtubules, and vimentin intermediate filaments cooperate for elongation of invadopodia. J Cell Biol 189, 541–556.

Soderberg E, Hessle V, von Euler A, Visa N (2012). Profilin is associated with transcriptionally active genes. Nucleus 3, 290–299.

Spradling AC (1993). Developmental genetics of oogenesis. In: The Development of Drosophila melanogaster, ed. B Martinez-Arias, Cold Spring Harbor, NY: Cold Spring Harbor Laboratory Press, 1–70.

Stark LA, Din FV, Zwacka RM, Dunlop MG (2001). Aspirin-induced activation of the NF-kappaB signaling pathway: a novel mechanism for aspirin-mediated apoptosis in colon cancer cells. FASEB J 15, 1273–1275.

Stark LA, Dunlop MG (2005). Nucleolar sequestration of RelA (p65) regulates NF-kappaB-driven transcription and apoptosis. Mol Cell Biol 25, 5985–6004.

Stuven T, Hartmann E, Gorlich D (2003). Exportin 6: a novel nuclear export receptor that is specific for profilin-actin complexes. EMBO J 22, 5928–5940.

Tamma G, Wiesner B, Furkert J, Hahm D, Oksche A, Schaefer M, Valenti G, Rosenthal W, Klussmann E (2003). The prostaglandin E2 analogue sulprostone antagonizes vasopressin-induced antidiuresis through activation of Rho. J Cell Sci 116, 3285–3294.

Technau M, Roth S (2008). The Drosophila KASH domain proteins Msp-300 and Klarsicht and the SUN domain protein klaroid have no essential function during oogenesis. Fly 2, 82–91.
Telley IA, Gaspar I, Ephrussi A, Surrey T (2012). Aster migration determines the length scale of nuclear separation in the Drosophila syncytial embryo. J Cell Biol 197, 887–895.
Thoms HC, Dunlop MG, Stark LA (2007). p38-mediated inactivation of cyclin D1/cyclin-dependent kinase 4 stimulates nucleolar translocation of RelA and apoptosis in colorectal cancer cells. Cancer Res 67, 1660–1669.
Tootle TL (2013). Genetic insights into the in vivo functions of prostaglandin signaling. Int J Biochem Cell Biol 45, 1629–1632.
Tootle TL, Spradling AC (2008). Drosophila Pxt: a cyclooxygenase-like facilitator of follicle maturation. Development 135, 839–847.
Verboon JM, Rincon-Arano H, Werwie TR, Delrow JJ, Scalzo D, Nandakumar V, Groudine M, Parkhurst SM (2015). Wash interacts with lamin and affects global nuclear organization. Curr Biol 25, 804–810.
Verheyen E, Cooley L (1994). Profilin mutations disrupt multiple actin-dependent processes during *Drosophila* development. Development 120, 717–728.
Vignjevic D (2006). Role of fascin in filopodial protrusion. J Cell Biol 174, 863–875.
Wheatley S, Kulkarni S, Karess R (1995). Drosophila nonmuscle myosin II is required for rapid cytoplasmic transport during oogenesis and for axial nuclear migration in early embryos. Development 121, 1937–1946.
Winkelman JD, Bilancia CG, Peifer M, Kovar DR (2014). Ena/VASP Enabled is a highly processive actin polymerase tailored to self-assemble parallel-bundled F-actin networks with Fascin. Proc Natl Acad Sci USA 111, 4121–4126.
Yoder BJ, Tso E, Skacel M, Pettay J, Tarr S, Budd T, Tubbs RR, Adams JC, Hicks DG (2005). The expression of fascin, an actin-bundling motility protein, correlates with hormone receptor-negative breast cancer and a more aggressive clinical course. Clin Cancer Res 11, 186–192.
Yu J, Starr DA, Wu X, Parkhurst SM, Zhuang Y, Xu T, Xu R, Han M (2006). The KASH domain protein MSP-300 plays an essential role in nuclear anchoring during Drosophila oogenesis. Dev Biol 289, 336–345.
Zanet J, Jayo A, Plaza S, Millard T, Parsons M, Stramer B (2012). Fascin promotes filopodia formation independent of its role in actin bundling. J Cell Biol 197, 477–486.
Zanet J, Stramer B, Millard T, Martin P, Payre F, Plaza S (2009). Fascin is required for blood cell migration during Drosophila embryogenesis. Development 136, 2557–-2565.
Zhang J, Fonovic M, Suyama K, Bogyo M, Scott MP (2009). Rab35 controls actin bundling by recruiting fascin as an effector protein. Science 325, 1250–1254.